Surface Plasmon Resonance (SPR) Theory: Tutorial
表面プラズモン共鳴の理論: チュートリアル

Masahiro Yamamoto
Department of Energy and Hydrocarbon Chemistry, Kyoto University,
Kyoto-Daigaku-Katsura, Nishikyo-ku, 615-8510, JAPAN
京都大学大学院工学研究科物質エネルギー化学専攻　山本雅博

October 20, 2008

1 Introduction

表面プラズモン共鳴 (SPR: Surface Plasmon Resonance) 法ではサブナノメーターオーダーの厚み (または屈折率）の変化を自作の安価な装置（He-Ne レーザー、回転ステージ、フォトダイオード、プリズム、Appendix 参照のこと）で簡単に測定できるために、抗原-抗体反応等を検出する免疫測定の分野を中心に広く用いられている。光学プリズム | 金属薄膜（通常は 50nm 厚み程度の金）| 試料系に光を入射すると、光と金表面の表面プラズマ振動[1] がカップルする特定の光入射角度で光の反射率がほぼゼロになる。この角度は、後述するように試料のサブナノメータの厚みの変化・屈折率変化に敏感に反応する。自動化された通常の測定・解析ルーチンでは共鳴角度のシフトの測定結果と理論式の数値計算から厚み・屈折率を求めればよいため原理を完全に理解する必要はないかもしれないが、装置をブラックボックスとして使用するのが心地よくない趣味人と実験データを詳細に解析して新たな知見を得ようとする者には原理の理解は不可欠であろう。

プラズモンという名前から量子力学的な取り扱いが必要であると誤解されるかもしれないが、SPR の原理は多層膜界面での光の反射・透過・吸収（すなわち完全に古典的な電磁気学・光学）の問題から説明できるものである。Raether の本 [1] にその原理は詳しく書いてあるが、あくまで専門家向けでありそれを理解するのは筆者にとって容易ではなかった。[2]。筆者はある事情から SPR 反射率曲線の解釈を行う必要性にせまられ[3] その原理を一から理解するために自習ノートを作成した。（英語?!で書いた部分。ホームページ http://fm.ehcc.kyoto-u.ac.jp に公開している。）今回このノートを Review of Polarography 誌の「ポイント解説」に掲載する機会を与えて頂き (”Review of Polarography, 48, No3. 2002, 209 ”)、それをもとに加筆訂正したのでここに報告する。筆者の英語力の不足から加筆・訂正部分は日本語であり、英語と日本語がミックスすることをご容赦願いたい。

また、本解説では SPR 法についての原理を考察する前に、誘電体界面での電磁波の反射・透過・吸収についても記述したので、エバネッセント波を用いた界面分光法、光反射法、エリプソメトリー、非線形分光学法等の電気化学界面系をフォトンイン-フォトンアウトで測定されている方々の理解にお役にたてれば幸いである。

The SPR(surface plasmon resonance)[2] is the century-old technique from the finding of the Wood’s anomaly for the reflected light from the diffraction gratings[3]. After

[1] プラズマ振動は、金属内の電子が集団的に運動して、正負の電荷がつりあっている位置から振動する現象である。表面プラズマ振動は表面・界面にのみ存在するプラズマ振動モードである。プラズモンはプラズマ振動を量子化した表現である。

[2] 栗原らの測定原理の解説（栗原、鈴木「ぶんせき」2002, 161.）もあるが、ここでは電磁気学の基礎方程式から SPR 共鳴条件式を導くことを試みる。

[3] Tell me, and I forget. Teach me, and I may remember. Involve me , and I learn. Benjamin Franklin

Otto's demonstration[4] for the surface plasmon excitation by light with attenuated-total-reflection(ATR) coupler[5], the SPR method applied to the organic films[6] or the detection of antigen-antibody reaction[7]. The SPR theory is also well established[1], and the recent advance in the measurements can be reported in the reviews[8, 9, 10].

In the SPR method the dielectric constant change in the sub-nm region from the surface can be measured and the method can be easily applied to the adsorption phenomena **in the electrochemical environment**[11, 12], where the capacitance can be measured simultaneously and get the complementary information of the change in the dielectric properties on the electrode surface.

本解説で、電磁気学は砂川重信「理論電磁気学」(紀伊国屋書店, 1973)、光学は M. Born and E. Wolf "Principles of Optics (7th expanded edition)" (Cambridge Univ. Press, 1999)[13] および E. Hecht "Optics(4th edition)" (Addison Wesley, 2002)[14] を参考にした。

2 Maxwell Equation

The Maxwell equations are described [4]

$$\mathrm{div}\mathbf{D} = \rho \tag{1}$$

$$\mathrm{div}\mathbf{B} = 0 \tag{2}$$

$$\mathrm{rot}\mathbf{E} = -\frac{\partial \mathbf{B}}{\partial t} \tag{3}$$

$$\mathrm{rot}\mathbf{H} = \mathbf{J} + \frac{\partial \mathbf{D}}{\partial t} \tag{4}$$

Here we use MKSA-SI unit. The electric field $\mathbf{E}$ (Vm^{-1}) and magnetic field $\mathbf{H}$ (Am^{-1}) are related to the electric displacement (or dielectric flux density or electric flux density) $\mathbf{D}$ (Cm^{-2}) and magnetic-flux density (or magnetic induction) $\mathbf{B}$ (T:tesla = $\mathrm{NA}^{-1}\mathrm{m}^{-1}$)

$$\mathbf{D} = \epsilon\epsilon_0\mathbf{E} \tag{5}$$

$$\mathbf{B} = \mu\mu_0\mathbf{H} \tag{6}$$

Here ϵ and ϵ_0 are the dielectric constant (with no dimension) and electric permittivity of free space [8.854187817 $\times 10^{-12}$ Fm^{-1} (= $\mathrm{CV}^{-1}\mathrm{m}^{-1}$)], respectively. μ and μ_0 are magnetic permeability (with no dimension) and magnetic permeability of free space ($4\pi \times 10^{-7}$ NA^{-2}), respectively. We will assume the Ohm's law for the relation between the current $\mathbf{J}$ and the electric field $\mathbf{E}$

$$\mathbf{J} = \sigma\mathbf{E} \tag{7}$$

[4] マックスウェル方程式は電磁気学・光学の基礎方程式であり、非常に美しい形をいている。その物理的な意味は高校ですでにならっているが、それを3次元空間(時間を入れて4次元)に拡張したものである。マックスウェル方程式の導入は最近出版された竹内淳「高校数学でわかるマックスウェル方程式」(講談社ブルーバックス,2002) がわかりやすい。div$\mathbf{V}$ はベクトル場 $\mathbf{V}(\mathbf{r})$ の微少体積 $d\mathbf{r}$ での出入りの差(発散)を表す。ベクトル解析において、rot の意味はわかりにくいが、長沼伸一郎「物理数学の直感的方法」(通商産業研究社)の5章に記述されている水の流れに中においた微少な水車の回転速度という記述は大変わかりやすい。[The rotational velocity of the infinitesimal water wheel in water flow field $\mathbf{u}$. (The water flow of the right side of the wheel in the upper direction u_y is faster than the left side ($\partial u_y/\partial x > 0$), the wheel rotates in the anticlockwise direction. In the same the water flow of the upper side of the wheel in the right direction u_x is slower than the lower side ($\partial u_x/\partial y < 0$) the wheel rotates in the anticlockwise direction. $(\mathrm{rot}\mathbf{u})_z = \partial u_y/\partial x - \partial u_x/\partial y$)] マックスウェル方程式は、荒く表現するなら、Eq.(1):正(負)電荷から出(入)ていく電気力線の数はその電荷に比例する、Eq.(2):磁石はかならず SN 極をもつ、Eq.(3):コイルに磁石を近づけると磁場をうち消すような(従ってマイナス符号)誘導電流が流れる、Eq.(4):電線に電流を流すとその回りに(右ねじが進む方向に)回転磁場が発生する、ことを意味する。

2.1 Energy Conservation and Poynting Vector

The equation of motion of point charges is [5]

$$m_i \ddot{\mathbf{r}}_i = \int d\mathbf{r} \left\{ e_i \delta(\mathbf{r} - \mathbf{r}_i(t)) \mathbf{E} + e_i \delta(\mathbf{r} - \mathbf{r}_i(t)) \dot{\mathbf{r}}_i \times \mathbf{B} \right\}$$

If we apply $(\sum_i \mathbf{v}_i \cdot)$ from the left, and the velocity is defined as $\mathbf{v}_i = \dot{\mathbf{r}_i}$

$$\begin{aligned} \sum_i m_i \mathbf{v}_i \cdot \dot{\mathbf{v}}_i &= \sum_i \int d\mathbf{r} \left\{ e_i \delta(\mathbf{r} - \mathbf{r}_i(t)) \mathbf{v}_i \cdot \mathbf{E} + e_i \delta(\mathbf{r} - \mathbf{r}_i(t)) \underbrace{\mathbf{v}_i \cdot [\mathbf{v}_i \times \mathbf{B}]}_{=0} \right\} \\ &= \sum_i \int d\mathbf{r} e_i \delta(\mathbf{r} - \mathbf{r}_i(t)) \mathbf{v}_i \cdot \mathbf{E} \end{aligned} \tag{8}$$

From the definition of the current and the Eq.(4).

$$\mathbf{J} = \sum_i e_i \dot{\mathbf{r}}_i(t) \delta(\mathbf{r} - \mathbf{r}_i(t)) \tag{9}$$

$$= \mathrm{rot}\mathbf{H} - \frac{\partial \mathbf{D}}{\partial t} \tag{10}$$

Then

$$\sum_i \frac{d}{dt}\left(\frac{1}{2} m_i \mathbf{v}_i^2\right) = \int d\mathbf{r} \left(\mathrm{rot}\mathbf{H} - \frac{\partial \mathbf{D}}{\partial t}\right) \cdot \mathbf{E} \tag{11}$$

$$\begin{aligned} \frac{1}{2}\frac{\partial}{\partial t}(\mathbf{E}\cdot\mathbf{D} + \mathbf{B}\cdot\mathbf{H}) &= \mathbf{E}\cdot\frac{\partial \mathbf{D}}{\partial t} + \mathbf{H}\cdot\frac{\partial \mathbf{B}}{\partial t} \\ &= \mathbf{E}\cdot\frac{\partial \mathbf{D}}{\partial t} - \mathbf{H}\cdot\mathrm{rot}\mathbf{E} \\ \frac{d}{dt}\left(\sum_i \frac{1}{2} m_i \mathbf{v}_i^2\right) &= \int d\mathbf{r} \left[-\frac{1}{2}\frac{\partial}{\partial t}(\mathbf{E}\cdot\mathbf{D} + \mathbf{B}\cdot\mathbf{H}) \right. \\ &\qquad \left. \underbrace{-\mathbf{H}\cdot\mathrm{rot}\mathbf{E} + \mathbf{E}\cdot\mathrm{rot}\mathbf{H}}_{=-\mathrm{div}(\mathbf{E}\times\mathbf{H})} \right] \end{aligned}$$

$$\frac{d}{dt}\left[\underbrace{\sum_i \frac{1}{2} m_i \mathbf{v}_i^2}_{\text{kinetic energy}} + \underbrace{\frac{1}{2}\int d\mathbf{r}(\mathbf{E}\cdot\mathbf{D} + \mathbf{B}\cdot\mathbf{H})}_{\text{total energy of electromagnetic field}} \right] = -\int dS \underbrace{[\mathbf{E}\times\mathbf{H}]}_{\text{Poynting vector}} \cdot \mathbf{n} \tag{12}$$

From above equations the Poynting vector $\mathbf{S}[= \mathbf{E}\times\mathbf{H}]$ means the energy flux going out from the system.

2.2 Wave Equations

From Eqs.(3) and (6)

$$\mathrm{rot}\mathbf{E} = -\mu\mu_0 \frac{\partial \mathbf{H}}{\partial t} \tag{13}$$

[5] δ関数で与えられる点電荷は、電場・磁場からローレンツ力を受ける。

From Eqs.(4), (5), and (7)

$$\text{rot}\mathbf{H} = \sigma\mathbf{E} + \epsilon\epsilon_0\frac{\partial \mathbf{E}}{\partial t} \tag{14}$$

If we apply $\nabla\times$ to Eq.(13) and $\partial/\partial t$ to Eq.(14) and using the relation

$$\begin{aligned}
\nabla\times\nabla\times\mathbf{E} &= \text{rot}\begin{vmatrix} \mathbf{i} & \mathbf{j} & \mathbf{k} \\ \frac{\partial}{\partial x} & \frac{\partial}{\partial y} & \frac{\partial}{\partial z} \\ E_x & E_y & E_z \end{vmatrix} = \begin{vmatrix} \mathbf{i} & \mathbf{j} & \mathbf{k} \\ \frac{\partial}{\partial x} & \frac{\partial}{\partial y} & \frac{\partial}{\partial z} \\ \frac{\partial E_z}{\partial y} - \frac{\partial E_y}{\partial z} & \frac{\partial E_x}{\partial z} - \frac{\partial E_z}{\partial x} & \frac{\partial E_y}{\partial x} - \frac{\partial E_x}{\partial y} \end{vmatrix} \\
&= \mathbf{i}\left[\frac{\partial^2 E_y}{\partial x\partial y} - \frac{\partial^2 E_x}{\partial y^2} - \frac{\partial^2 E_x}{\partial z^2} + \frac{\partial^2 E_z}{\partial x\partial z}\right] + \mathbf{j}[..] + \mathbf{k}[..] \\
&= \mathbf{i}\frac{\partial}{\partial x}\left(\frac{\partial E_x}{\partial x} + \frac{\partial E_y}{\partial y} + \frac{\partial E_z}{\partial z}\right) + \mathbf{j}\frac{\partial}{\partial y}\text{div}\mathbf{E} + \mathbf{k}\frac{\partial}{\partial z}\text{div}\mathbf{E} \\
&\quad -\mathbf{i}\nabla^2 E_x - \mathbf{j}\nabla^2 E_y - \mathbf{k}\nabla^2 E_z \\
&= \text{grad}(\text{div}\mathbf{E}) - \nabla^2\mathbf{E} \qquad (15)
\end{aligned}$$

If we assume $\rho = 0$, $\text{div}\mathbf{E} = 0$ then

$$\nabla^2\mathbf{E} = \sigma\mu\mu_0\frac{\partial \mathbf{E}}{\partial t} + \mu\mu_0\epsilon\epsilon_0\frac{\partial^2\mathbf{E}}{\partial t^2} \tag{16}$$

In the same way we can get

$$\nabla^2\mathbf{H} = \sigma\mu\mu_0\frac{\partial \mathbf{H}}{\partial t} + \mu\mu_0\epsilon\epsilon_0\frac{\partial^2\mathbf{H}}{\partial t^2} \tag{17}$$

In the case that the electric field has a plane wave form

$$\mathbf{E} = \mathbf{E}_0 e^{i(\mathbf{k}\cdot\mathbf{r} - \omega t)} \tag{18}$$

where $\mathbf{E}_0$ is the polarization vector and the wavevector $\mathbf{k}$ is in the direction of the wave propagation and the magnitude is given from Eq.(16)

$$k^2 = i\sigma\mu\mu_0\omega + \mu\mu_0\epsilon\epsilon_0\omega^2 \tag{19}$$

In vacuum, $\epsilon = 1, \mu = 1, \sigma = 0$ and $c/\nu = \lambda, c/\omega = \lambda/(2\pi), k = 2\pi/\lambda = \omega/c$ then

$$c = 1/\sqrt{\mu_0\epsilon_0} \tag{20}$$

The complex optical index $\tilde{n}$ may be given by

$$k = \frac{2\pi}{\lambda} = \frac{\omega}{v} = \frac{\tilde{n}\omega}{c} \tag{21}$$

$$\tilde{n}^2 = k^2c^2/\omega^2 = \mu\epsilon + i\frac{\sigma\mu}{\epsilon_0\omega} \tag{22}$$

$$\tilde{n} = n + i\kappa, \quad k = \tilde{n}\omega/c = (n + i\kappa)\omega/c \tag{23}$$

where n and κ are the real and imaginary part of the complex optical index, respectively.

$$\begin{aligned}
E(z,t) &= E_0 e^{i(kz-\omega t)} = E_0 e^{-\kappa\omega z/c} e^{i(n\omega z/c - \omega t)} && (24) \\
I(z) &\propto E^*E = |E_0|^2 e^{-2\kappa\omega z/c} = I_0 e^{-\alpha z} \qquad (\text{Lambert's Law}) \\
\alpha &= 2\kappa\omega/c && (25) \\
\tilde{n}^2 &= \tilde{\epsilon} = \epsilon_1 + i\epsilon_2 \qquad [\mu = 1, \sigma = 0 \text{ in Eq.(22)}] && (26) \\
\epsilon_1 &= n^2 - \kappa^2, \quad \epsilon_2 = 2n\kappa && (27)
\end{aligned}$$

Here α is the absorption coefficient, $\tilde{\epsilon}$ is the complex dielectric constant, ϵ_1 and ϵ_2 are the real and imaginary part of the complex dielectric constant, respectively.

If we take divergence of the plane-wave electric filed,

$$\begin{aligned}
\mathrm{div}\mathbf{E} &= \left(\mathbf{i}\frac{\partial}{\partial x}+\mathbf{i}\frac{\partial}{\partial y}+\mathbf{i}\frac{\partial}{\partial z}\right)\cdot(E_{0x}\mathbf{i}+E_{0y}\mathbf{j}+E_{0z}\mathbf{k})e^{i(k_x x+k_y y+k_z z-\omega t)} && (28)\\
&= i(k_x E_{0x}+k_y E_{0y}+k_z E_{0z}) = i\mathbf{k}\cdot\mathbf{E}_0 && (29)\\
&= \frac{\rho}{\epsilon_0\epsilon} = 0 && (30)
\end{aligned}$$

Then we can find that the electric field is transverse wave, i.e. $\mathbf{k}\perp\mathbf{E}_0$.

If the magnetic-flux density $\mathbf{B}$ is written as

$$\mathbf{B} = \frac{\mathbf{k}\times\mathbf{E}_0}{\omega}e^{i(\mathbf{k}\cdot\mathbf{r}-\omega t)}, \tag{31}$$

then the magnetic-flux density satisfies Eq.(3), because

$$\begin{aligned}
\mathrm{rot}\mathbf{E} &= \mathbf{i}\left(\frac{\partial E_z}{\partial y}-\frac{\partial E_y}{\partial z}\right)+.. && (32)\\
&= \mathbf{i}(ik_y E_z - ik_z E_y)+.. && (33)\\
&= i\mathbf{k}\times\mathbf{E} && (34)\\
-\frac{\partial\mathbf{B}}{\partial t} &= -\frac{\mathbf{k}\times\mathbf{E}_0}{\omega}(-i\omega)e^{i(\mathbf{k}\cdot\mathbf{r}-\omega t)} && (35)\\
&= i\mathbf{k}\times\mathbf{E} && (36)
\end{aligned}$$

In vacuum

$$\frac{|\mathbf{E}_0|}{|\mathbf{H}_0|} = \frac{\mu_0\omega}{k} = \frac{\mu_0\omega}{\sqrt{\epsilon_0\mu_0}\omega} = \sqrt{\frac{\mu_0}{\epsilon_0}} = 376.7\ \Omega \tag{37}$$

2.3 Boundary Conditions at a Interface Between Different Media

Now we think a interface which is at the boundary medium 1 and 2 as shown in Fig.1. From Gauss law, we can get the following for the Gauss box which include the interface inside the box,

$$\int_V d\mathbf{r}\underbrace{\nabla\cdot\mathbf{D}}_{\rho} = \int_S \mathbf{D}\cdot d\mathbf{S} \tag{38}$$

In the limit that the Gauss box is very thin ($\delta h\to 0$)

$$\int_V d\mathbf{r}\rho = Q_{\mathrm{box}} = \mathbf{n}\cdot[\mathbf{D}_1-\mathbf{D}_2]S \tag{39}$$

where vector $\mathbf{n}$ means the surface normal unit vector pointing from media 2 to 1.

$$\mathbf{n}\cdot[\mathbf{D}_1-\mathbf{D}_2] = Q_{\mathrm{box}}/S = \sigma_{12} \tag{40}$$

where σ_{12} means the interface charge density. From $\nabla\cdot\mathbf{B}=0$

$$\mathbf{n}\cdot[\mathbf{B}_1-\mathbf{B}_2] = 0 \tag{41}$$

As shown in Fig. 2 for a general vector field $\mathbf{V}(\mathbf{r})$, Stokes theorem gives

$$\begin{aligned}
\oint\mathbf{V}\cdot d\mathbf{r} &= (\mathrm{I})+(\mathrm{II})+(\mathrm{III})+(\mathrm{IV})\\
&= V_x(x_0,y_0)dx+V_y(x_0+dx,y_0)dy+V_x(x_0,y_0+dy)(-dx)+V_y(x_0,y_0)(-dy)
\end{aligned}$$

$$
\begin{aligned}
&= V_x(x_0,y_0)dx + [V_y(x_0,y_0) + \frac{\partial V_y}{\partial x}dx]dy \\
&\quad -[V_x(x_0,y_0) + \frac{\partial V_x}{\partial y}dy]dx - V_y(x_0,y_0)dy \\
&= \left(\frac{\partial V_y}{\partial x} - \frac{\partial V_x}{\partial y}\right) dxdy = (\mathrm{rot}\mathbf{V})_z dxdy
\end{aligned}
$$

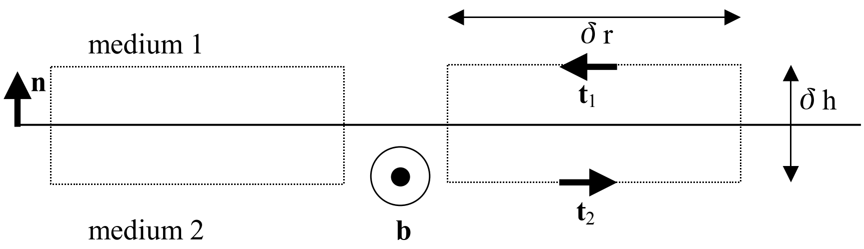

Figure 1: Gauss and Stokes box

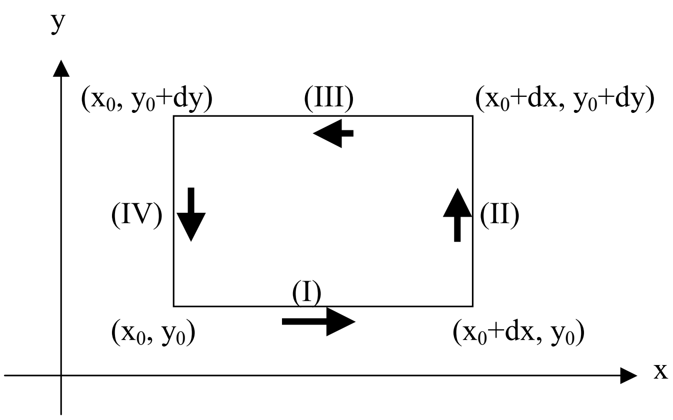

Figure 2: Stokes theorem

From Eq.(3) and Stokes theorem we can get

$$\oint_C \mathbf{E}\cdot d\mathbf{r} = \int_S \mathrm{rot}\mathbf{E}\cdot d\mathbf{S} \tag{42}$$

$$= -\int_S \frac{\partial \mathbf{B}}{\partial t}\cdot \mathbf{b}dS \tag{43}$$

$$\delta r[\mathbf{E}_1\cdot\mathbf{t}_1 + \mathbf{E}_2\cdot\mathbf{t}_2] = -\frac{\partial \mathbf{B}}{\partial t}\cdot\mathbf{b}\delta r\delta h \longrightarrow 0 \tag{44}$$

$$\mathbf{t} = \mathbf{t}_1 = -\mathbf{t}_2 \tag{45}$$

$$\mathbf{t}\cdot[\mathbf{E}_1 - \mathbf{E}_2] = 0 \tag{46}$$

Here $\mathbf{b}$ is the unit vector defined by $\mathbf{b} = \mathbf{n}\times\mathbf{t}$. From Eq.(4)

$$\oint_C \mathbf{H}\cdot d\mathbf{r} = \int_S \mathrm{rot}\mathbf{H}\cdot d\mathbf{S} \tag{47}$$

$$= \int_S \left(\mathbf{J} + \frac{\partial \mathbf{D}}{\partial t}\right)\cdot\mathbf{b}dS \tag{48}$$

$$\delta r[\mathbf{H}_1 \cdot \mathbf{t}_1 + \mathbf{H}_2 \cdot \mathbf{t}_2] = \left(\mathbf{J} + \frac{\partial \mathbf{D}}{\partial t}\right) \cdot \mathbf{b}\delta r \delta h \longrightarrow \mathbf{J} \cdot \mathbf{b}\delta r \delta h \quad (49)$$

$$\mathbf{t} \cdot [\mathbf{H}_1 - \mathbf{H}_2] = \mathbf{J}_s \quad [\equiv \text{surface current density}(\mathrm{Am}^{-1})] \quad (50)$$

3 Reflection and Transmission

Now we define the incident plane wave as

$$\mathbf{E} = \mathbf{E}_0 e^{i(\mathbf{k}\cdot\mathbf{r}-\omega t)}, \quad \omega = \omega(k), \quad \mathbf{B} = \frac{\mathbf{k} \times \mathbf{E}_0}{\omega} e^{i(\mathbf{k}\cdot\mathbf{r}-\omega t)} \quad (51)$$

reflected wave as

$$\mathbf{E}' = \mathbf{R}_0 e^{i(\mathbf{k}'\cdot\mathbf{r}-\omega' t)}, \quad \omega' = \omega'(k'), \quad \mathbf{B}' = \frac{\mathbf{k}' \times \mathbf{R}_0}{\omega'} e^{i(\mathbf{k}'\cdot\mathbf{r}-\omega' t)} \quad (52)$$

transmitted wave as

$$\mathbf{E}'' = \mathbf{T}_0 e^{i(\mathbf{k}''\cdot\mathbf{r}-\omega'' t)}, \quad \omega'' = \omega''(k''), \quad \mathbf{B}'' = \frac{\mathbf{k}'' \times \mathbf{T}_0}{\omega''} e^{i(\mathbf{k}''\cdot\mathbf{r}-\omega'' t)} \quad (53)$$

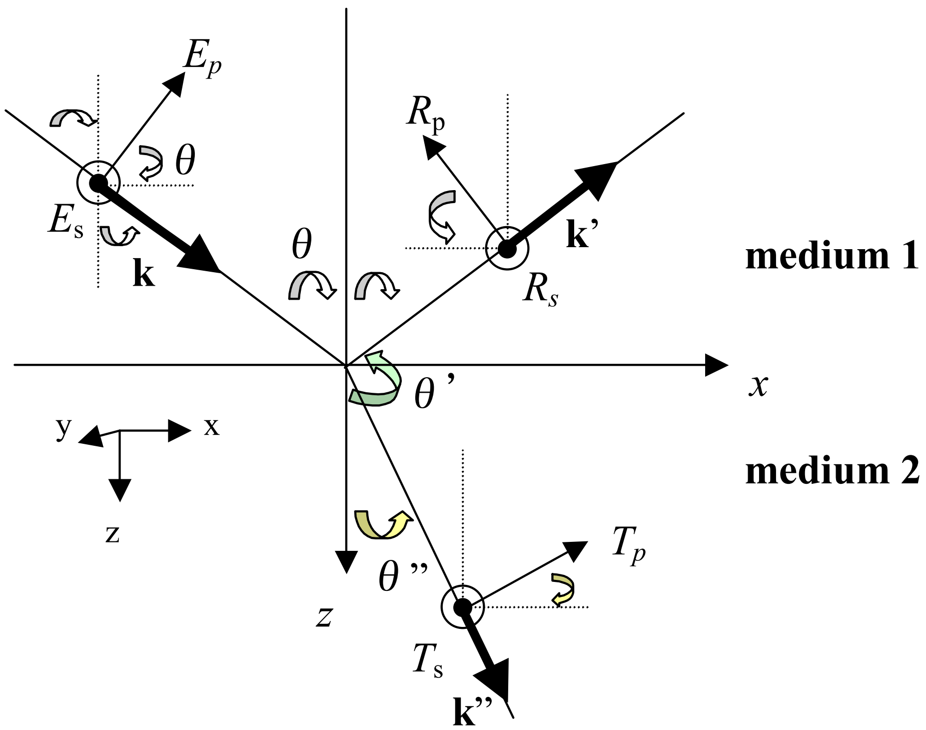

Figure 3: Reflection and Transmission of Light

From Fig.3

$$\mathbf{k} = (k\sin\theta, 0, k\cos\theta) \quad (54)$$

$$\mathbf{k}' = (k'\sin\theta', 0, k'\cos\theta'), \qquad e^{i(\pi-\theta')} = -\cos\theta' + i\sin\theta' \quad (55)$$

$$\mathbf{k}'' = (k''\sin\theta'', 0, k''\cos\theta'') \quad (56)$$

The p-wave has the components of x and z, but s-wave has only the y component. [6]

[6] 光（電磁場）は横波であるので、光の進行方向に対して２つの偏光成分を持つ。（デジタル腕時計の液晶

3.1 Condition I: $\mathbf{t}\cdot[\mathbf{E}_1-\mathbf{E}_2]=0$

From Eq.(46) the tangential component of the electric field become

$$\begin{aligned} E_x + E'_x &= E''_x \quad \text{at } z=0 && (57)\\ E_p\cos\theta e^{i(k\sin\theta x-\omega t)} + R_p\cos\theta' e^{i(k'\sin\theta' x-\omega' t)} &= T_p\cos\theta'' e^{i(k''\sin\theta'' x-\omega'' t)} && (58)\end{aligned}$$

For any x at $z=0$ this condition should be satisfied, then

$$\begin{aligned} \omega &= \omega' = \omega'' && (59)\\ k\sin\theta &= k'\sin\theta' = k''\sin\theta'' && (60)\end{aligned}$$

The magnitude of the wavevector is given by Eq.(21)

$$\sin\theta = \sin\theta' = \sin(\pi-\theta'), \quad \text{because} \;\; k=k' \tag{61}$$

The incident angle equals to the reflection angle, and

$$k\sin\theta = \tilde{n}_1\frac{\omega}{c}\sin\theta = k''\sin\theta'' = \tilde{n}_2\frac{\omega''}{c}\sin\theta'' \tag{62}$$

Then we can get **Snell's law** because $\omega=\omega''$

$$\tilde{n}_1\sin\theta = \tilde{n}_2\sin\theta'' \tag{63}$$

The Eq.(58) becomes

$$(E_p - R_p)\cos\theta = T_p\cos\theta'' \tag{64}$$

From Fig.3 we can get

$$\mathbf{E}_0 = \begin{pmatrix} E_p\cos\theta \\ E_s \\ -E_p\sin\theta \end{pmatrix}, \mathbf{R}_0 = \begin{pmatrix} -R_p\cos\theta \\ R_s \\ -R_p\sin\theta \end{pmatrix}, \mathbf{T}_0 = \begin{pmatrix} T_p\cos\theta'' \\ T_s \\ -T_p\sin\theta'' \end{pmatrix} \tag{65}$$

For y-direction we can get the condition

$$\begin{aligned} E_y + E'_y &= E''_y \quad \text{at } z=0 && (66)\\ (E_s+R_s)e^{i(k\sin\theta x-\omega t)} &= T_s e^{i(k''\sin\theta'' x-\omega t)} && (67)\\ (E_s+R_s) &= T_s && (68)\end{aligned}$$

3.2 Condition II: $\mathbf{n}\cdot(\mathbf{B}_1-\mathbf{B}_2)=0$

For the boundary condition in Eq.(41)

$$\begin{aligned} \mathbf{k}\times\mathbf{E}_0 &= \begin{vmatrix} \mathbf{i} & \mathbf{j} & \mathbf{k} \\ k\sin\theta & 0 & k\cos\theta \\ E_p\cos\theta & E_s & -E_p\sin\theta \end{vmatrix} \\ &= k[-\mathbf{i}E_s\cos\theta + \mathbf{j}(E_p\cos^2\theta + E_p\sin^2\theta) + \mathbf{k}E_s\sin\theta] && (69)\\ \omega\mathbf{B} = \mathbf{k}\times\mathbf{E}_0 &= \begin{pmatrix} -kE_s\cos\theta \\ kE_p \\ kE_s\sin\theta \end{pmatrix} && (70)\end{aligned}$$

表示板 (ほぼ直線偏光?）を偏光サングラスで見ながら回転させると 90 °毎に明暗が見える。）**s 波（s 偏光）**は界面に平行な成分で、**p 波（p 偏光）**は s 波に垂直な成分である。電場成分が紙面に垂直なので s 波は **TE** (transverse electric) wave，磁場成分が紙面に垂直なので p 波は **TM** (transverse magnetic) wave とも言われる。

$$\mathbf{k}' \times \mathbf{R}_0 = \begin{vmatrix} \mathbf{i} & \mathbf{j} & \mathbf{k} \\ k\sin\theta & 0 & -k\cos\theta \\ -R_p\cos\theta & R_s & -R_p\sin\theta \end{vmatrix}$$

$$= k[\mathbf{i}R_s\cos\theta + \mathbf{j}(R_p\cos^2\theta + R_p\sin^2\theta) + \mathbf{k}R_s\sin\theta] \quad (71)$$

$$\omega\mathbf{B}' = \mathbf{k}' \times \mathbf{R}_0 = \begin{pmatrix} kR_s\cos\theta \\ kR_p \\ kR_s\sin\theta \end{pmatrix} \quad (72)$$

$$\mathbf{k}'' \times \mathbf{T}_0 = \begin{vmatrix} \mathbf{i} & \mathbf{j} & \mathbf{k} \\ k''\sin\theta'' & 0 & k''\cos\theta'' \\ T_p\cos\theta'' & T_s & -T_p\sin\theta'' \end{vmatrix}$$

$$= k''[-\mathbf{i}T_s\cos\theta'' + \mathbf{j}(T_p\cos^2\theta + T_p\sin^2\theta'') + \mathbf{k}T_s\sin\theta''] \quad (73)$$

$$\omega\mathbf{B}'' = \mathbf{k}'' \times \mathbf{T}_0 = \begin{pmatrix} -k''T_s\cos\theta'' \\ k''T_p \\ k''T_s\sin\theta'' \end{pmatrix} \quad (74)$$

The boundary condition $B_z + B'_z = B''_z$ becomes

$$\frac{k\sin\theta}{\omega}(E_s + R_s)e^{i(k\sin\theta x - \omega t)} = \frac{k''\sin\theta''}{\omega}T_s e^{i(k''\sin\theta'' x - \omega t)} \quad (75)$$

$$\tilde{n_1}(E_s + R_s)\sin\theta = \tilde{n_2}T_s\sin\theta'' \quad (76)$$

$$E_s + R_s = T_s \quad (77)$$

We used Snell's law in the last equation. This equation is the same as Eq.(68).

3.3 Condition III: $\mathbf{n}\cdot(\mathbf{D}_1 - \mathbf{D}_2)$

For the boundary condition in Eq.(40)

$$\tilde{\epsilon_1}\epsilon_0(E_z + E'_z) = \tilde{\epsilon_2}\epsilon_0 E''_z + \sigma_{12} \quad (78)$$

$$\tilde{\epsilon_1}\epsilon_0(-E_p\sin\theta - R_p\sin\theta)e^{i(k\sin\theta x - \omega t)} = \tilde{\epsilon_2}\epsilon_0(-T_p\sin\theta'')e^{i(k''\sin\theta'' x - \omega t)} + \sigma_{12}(\mathbf{r}, t)$$

$$\sigma_{12}(\mathbf{r}, t) = \delta(z)\int_{-\infty}^{\infty} dk \int_{-\infty}^{\infty} d\omega\sigma_{12}(k, \omega)e^{i(kx - \omega t)} \quad (79)$$

In Eq.(79) we used the Fourier transformed charge density $\sigma_{12}(k, \omega)$. If we apply $(1/2\pi)^2 \int\int dxdte^{-i(k'x - \omega' t)}$, then we use $(1/4\pi^2)\int\int dxdte^{i(k\sin\theta x - k'x)}e^{-i(\omega - \omega')t} = \delta(k\sin\theta - k')\delta(\omega - \omega')$ and the above equations are held at $z = 0$

$$\tilde{\epsilon_1}\epsilon_0(-E_p\sin\theta - R_p\sin\theta)\delta(k\sin\theta - k')\delta(\omega - \omega') = -\tilde{\epsilon_2}\epsilon_0 T_p\sin\theta''\delta(k''\sin\theta'' - k')$$
$$\delta(\omega - \omega') + \int\int dk'''d\omega'''\sigma_{12}(k''', \omega''')\delta(k''' - k')\delta(\omega''' - \omega) \quad (80)$$

$$\tilde{n_1}^2(E_p + R_p)\sin\theta = \tilde{n_2}^2 T_p\sin\theta'' + \frac{\sigma_{12}(k\sin\theta, \omega)}{\epsilon_0} \quad (81)$$

$$\text{From Snell's law} \quad (82)$$

$$\tilde{n_1}(E_p + R_p) = \tilde{n_2}T_p + \frac{\sigma_{12}(k\sin\theta, \omega)}{\epsilon_0\tilde{n_1}\sin\theta} \quad (83)$$

Here we can neglect the $\sigma_{12}(k\sin\theta, \omega)$ term [7].

[7] Laser light(10 mW He-Ne, focused to 20 μm, 10^{26} photons/s/m^2 = $I/(\hbar\omega)$ $I = c\epsilon_0 E_0^2/2$ (J/m^2/s = W/m^2) c=299792458 m, $E_0 = 1.5 \times 10^5$ V/m) Bright sunlight (average 480nm, 10^{18} photons/s/m^2

3.4 Condition IV: $\mathbf{t} \cdot [\mathbf{H}_1 - \mathbf{H}_2] = \mathbf{J}_s$

$$H_x + H'_x = H''_x + (J_s)_x \tag{84}$$
$$H_y + H'_y = H''_y + (J_s)_y \tag{85}$$
$$B_x = \mu\mu_0 H_x, ... \tag{86}$$
$$[J_s(\mathbf{r},t)]_x = \int\int dk d\omega [J_s(k,\omega)]_x e^{i(kx-\omega t)}, .. \tag{87}$$
$$\left(-\frac{kE_s\cos\theta}{\mu_1\mu_0\omega} + \frac{kR_s\cos\theta}{\mu_1\mu_0\omega}\right) e^{i(k\sin\theta x-\omega t)} = -\frac{k''T_s\cos\theta''}{\mu_2\mu_0\omega} e^{i(k''\sin\theta''-\omega t)} + [J_s(\mathbf{r},t)]_x$$
$$\frac{\tilde{n_1}\cos\theta}{\mu_1}(E_s - R_s) = \frac{\tilde{n_2}\cos\theta''}{\mu_2} T_s + c\mu_0[J_s(k\sin\theta,\omega)]_x \tag{88}$$
$$\left(\frac{kE_p}{\mu_1\mu_0\omega} + \frac{kR_p}{\mu_1\mu_0\omega}\right) e^{i(k\sin\theta x-\omega t)} = \frac{k''T_p}{\mu_2\mu_0\omega} e^{i(k''\sin\theta'' x-\omega t)} + [J_s(\mathbf{r},t)]_y \tag{89}$$
$$\frac{\tilde{n_1}}{\mu_1}(E_p + R_p) = \frac{\tilde{n_2}}{\mu_2} T_p + c\mu_0[J_s(k\sin\theta,\omega)]_y \tag{90}$$

3.5 Reflection and Transmission Coefficients

In the end we can obtain the following equation for p-wave

$$(E_p - R_p)\cos\theta = T_p\cos\theta'' \tag{91}$$
$$\tilde{n_1}(E_p + R_p) = \tilde{n_2} T_p + \frac{\sigma_{12}(k\sin\theta,\omega)}{\epsilon_0\tilde{n_1}\sin\theta} \tag{92}$$
$$\frac{\tilde{n_1}}{\mu_1}(E_p + R_p) = \frac{\tilde{n_2}}{\mu_2} T_p + c\mu_0[J_s(k\sin\theta,\omega)]_y \tag{93}$$

and for s-wave

$$E_s + R_s = T_s \tag{94}$$
$$\frac{\tilde{n_1}\cos\theta}{\mu_1}(E_s - R_s) = \frac{\tilde{n_2}\cos\theta''}{\mu_2} T_s + c\mu_0[J_s(k\sin\theta,\omega)]_x \tag{95}$$

3.5.1 Usual Solution: No Absorption in the Media 1 and 2.

Here we assume that $\sigma_{12}(k\sin\theta,\omega) = 0$, $\mathrm{Im}(\tilde{n}_{1,2}) = 0$ (later we will consider the case that the optical constant is complex, i.e. the medium absorb the light.), $\mu_1 = \mu_2 = 1$, $[J_s(k\sin\theta,\omega)]_x = 0$, $[J_s(k\sin\theta,\omega)]_y = 0$. Then for p-wave we can get

$$(E_p - R_p)\cos\theta = T_p\cos\theta'' \tag{96}$$
$$n_1(E_p + R_p) = n_2 T_p \tag{97}$$

and for s-wave

$$E_s + R_s = T_s \tag{98}$$
$$n_1\cos\theta(E_s + R_s) = n_2\cos\theta'' T_s \tag{99}$$

$E_0 = 18$V/m.) For electrochemical systems $\sigma_{12}(k\sin\theta = 0, \omega = 0)$ is the order of 10 μC/cm^2= 0.1 C/m^2 (fully dissociated 3-mercaptopropionic acid in the $\sqrt{3}\times\sqrt{3}$ structure on Au(111) surface = 0.74 C/m^2). $\sigma_{12}/\epsilon_0 = (1\sim 8)\times 10^{10}$ V/m. However, the surface charge at the electrode in the $\omega = 0$ limit do not couple to the photon field at $\omega = \omega_{\mathrm{photon}}$.

If we define the **amplitude reflection coefficient** r and the **amplitude transmission coefficient** for s- and p-waves,

$$r_p \equiv \frac{R_p}{E_p} \quad (100)$$

$$t_p \equiv \frac{T_p}{E_p} \quad (101)$$

$$r_s \equiv \frac{R_s}{E_s} \quad (102)$$

$$t_s \equiv \frac{T_s}{E_s} \quad (103)$$

$$(1 - r_p)\cos\theta = t_p \cos\theta'' \quad (104)$$

$$n_1(1 + r_p) = n_2 t_p \quad (105)$$

$$(106)$$

and for s-wave

$$1 + r_s = t_s \quad (107)$$

$$n_1 \cos\theta(1 - r_s) = n_2 \cos\theta'' t_s \quad (108)$$

We finally get the **Fresnel**(フレネル) equations

$$r_p = \frac{-n_1\cos\theta'' + n_2\cos\theta}{n_1\cos\theta'' + n_2\cos\theta} \quad (109)$$

$$t_p = \frac{2n_1\cos\theta}{n_1\cos\theta'' + n_2\cos\theta} \quad (110)$$

$$r_s = \frac{n_1\cos\theta - n_2\cos\theta''}{n_1\cos\theta + n_2\cos\theta''} \quad (111)$$

$$t_s = \frac{2n_1\cos\theta}{n_1\cos\theta + n_2\cos\theta''} \quad (112)$$

The reflectance R is defined as the ratio of the reflected power (or flux) to the incident power of the light

$$R = \frac{I' A\cos\theta'}{IA\cos\theta} = \frac{I'}{I} = \frac{n_1 R^2/(2c\mu_0)}{n_1 E^2/(2c\mu_0)} = r^2 \quad (113)$$

The radiant flux density I (W/m^2) is given by the averaged Poynting vector $<\mathbf{E}\times\mathbf{H}>= \tilde{n}E^2/(2c\mu_0)$. In the same way **the transmittance T may be given by**

$$T = \frac{I'' A\cos\theta''}{IA\cos\theta} = \frac{v_t\epsilon_t T^2\cos\theta''}{v_i\epsilon_i E^2\cos\theta} = \frac{n_2\cos\theta''}{n_1\cos\theta} t^2 \quad (114)$$

In Fig.4 and Fig.5 the r, t, R, and T are plotted for the air(1)|water(2) [air→water] and water(1)|air(2) [water→air] interface, respectively. [8] In the both cases t_s and t_p are

[8] Fig.5 の右側の図より水面からの反射光はすべての角度で s 波の方が強く散乱されることがわかる。従って、s 波をカットするように偏光サングラスがセットアップされていることが望ましい。s 波は、水平方向の電場ベクトルをもつ波である。従って、偏光サングラスは鉛直方向の電場ベクトルをもつ光を通すように作られている。水面からの反射光を偏光サングラスを通してみると、通常かける方向で光は最小になり、９０度めがね（もしよければ頭を！）回転すると反射光が最大になるのが観測される。LCD(liquid crystaldisplay) や液晶をつかった時計・表示板をみると、右方向に 45 度回すと真っ暗になる。偏光面を 45 度にして偏光サングラスをかけても見えるようにしているようだ。

また、水面 | 空気界面からの散乱では、後に示すように 48.66 °以上では全反射（反射率=1、透過率=0）する。

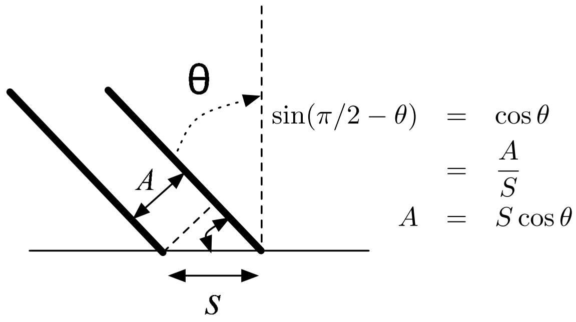

Figure 4: Angle dependency of the intensity of light

always positive, and this means the phase shifts of transmitted wave are always zero. For the case of air(1)|water(2) [air→water] r_s is always negative and r_p is positive for $\theta < \theta_{p,air\to water}$ and become negative for $\theta > \theta_{p,air\to water}$. These means that the phase shift is π for reflected s wave and phase shift become 0 to π at $\theta_{p,air\to water}$. For the case of water(1)|air(2) [water→air] r_s is always positive and r_p is negative for $\theta < \theta_{p,water\to air}$ and become positive for $\theta > \theta_{p,water\to air}$. These means that the phase shift is 0 for reflected s wave and phase shift become π to 0 at $\theta_{p,water\to air}$. In Appnedix the plot of the phase shift of the reflected s and p waves are shown. We also shown the condition of the **black film** formation in Appendix.

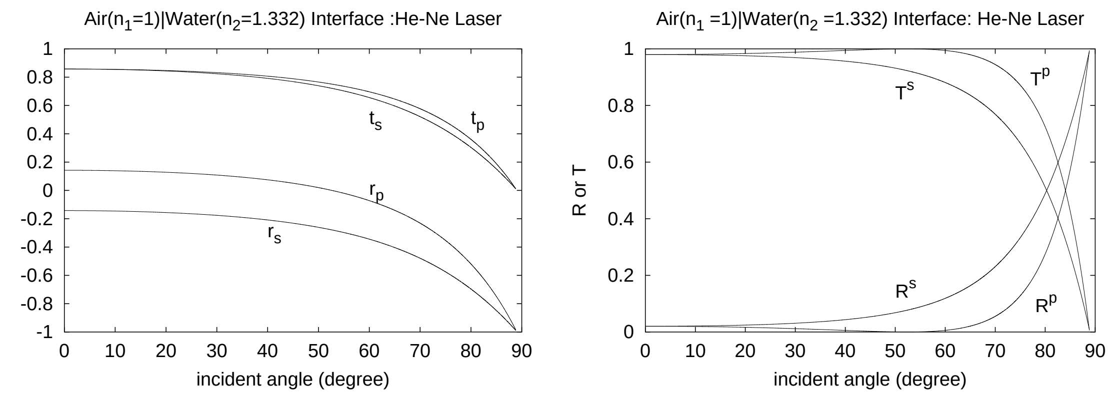

Figure 5: Reflection and transmission of He-Ne laser light at air|water interface

3.5.2 Brewster angle

In Figs.4 and 5, we can find the point $r_p = R^p = 0$ [9]and this condition is given by

$$-n_1\cos\theta'' + n_2\cos\theta = -n_1\left(\cos\theta'' - \frac{\sin\theta}{\sin\theta''}\cos\theta\right) = 0 \tag{115}$$

$$(\cos\theta''\sin\theta'' - \cos\theta\sin\theta) = \frac{e^{i\theta''}+e^{-i\theta''}}{2}\frac{e^{i\theta''}-e^{-i\theta''}}{2i} - \frac{e^{i\theta}+e^{-i\theta}}{2}\frac{e^{i\theta}-e^{-i\theta}}{2i}$$

[9] レーザー共振器内に,Brewster 角に設定したシリカ板を置けば p 偏光は反射されずに透過するが、s 偏光は行き帰りで２回反射されるために減衰する。

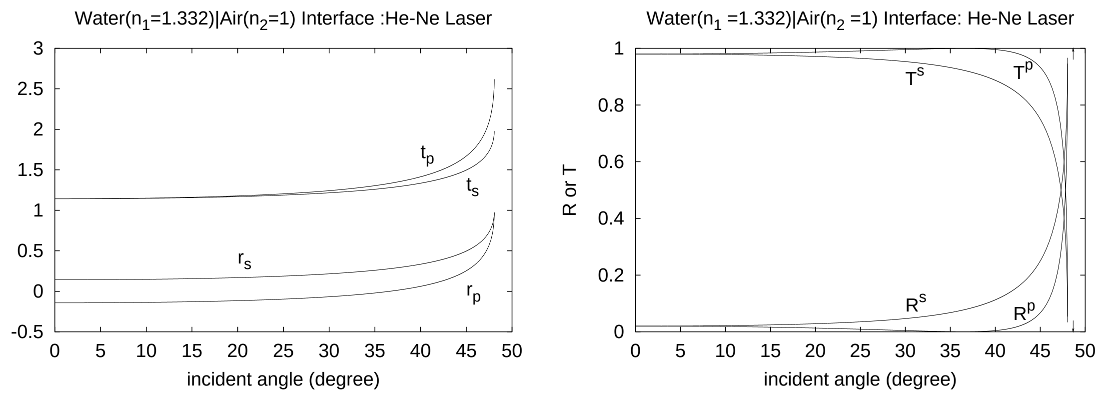

Figure 6: Reflection and transmission of He-Ne laser light at water|air interface

$$= \frac{e^{2i\theta''} - e^{-2i\theta''}}{4i} - \frac{e^{2i\theta} - e^{-2i\theta}}{4i}$$
$$= \frac{2i\sin(2\theta'') - 2i\sin(2\theta)}{4i} = 0$$

Then

$$\theta'' = \frac{\pi}{2} - \theta \tag{116}$$

The angle between the reflected light and the transmitted light is orthogonal.

$$n_2 \sin\theta'' = n_2 \sin(\pi/2 - \theta) = n_2 \cos\theta = n_1 \sin\theta \tag{117}$$

$$\theta_{\text{Brewster}} = \tan^{-1}\left(\frac{n_2}{n_1}\right) \tag{118}$$

From air to water reflection, the Brewster angle is 53.10 degree, and from water to air the angle is 36.90 degree.

3.6 Total Internal Reflection

Now we will consider the case that the angle θ'' between the transmitted wave and the surface normal is 90 degree, i.e., $\sin\theta''_c = (n_1/n_2)\sin\theta_c = 1$. Here

$$\theta_c = \sin^{-1}\frac{n_2}{n_1} \tag{119}$$

and should $n_2 < n_1$. For water to air reflection $\theta_c = 48.66$ degree. In this situation the transmitted light is along the surface parallel direction. What happens if $\theta > \theta_c$?

$$\cos\theta'' = \sqrt{1 - \sin^2\theta''} = i\sqrt{\sin^2\theta'' - 1} = i\sqrt{(n_1/n_2)^2\sin^2\theta - 1} \tag{120}$$

The transmitted wave can be written as

$$\mathbf{E}'' = \mathbf{T}_0 e^{i(\mathbf{k}''\cdot\mathbf{r} - \omega'' t)} \tag{121}$$
$$= \mathbf{T}_0 e^{i(k''\sin\theta'' x + k''\cos\theta'' z - \omega'' t)} \tag{122}$$
$$= \mathbf{T}_0 e^{i(k''\sin\theta'' x - \omega'' t)} e^{-k''\sqrt{(n_1/n_2)^2\sin^2\theta - 1}z} \tag{123}$$
$$= \mathbf{T}_0 e^{i\frac{n_2\omega\sin\theta''}{c}x} e^{-i\omega'' t} e^{-\frac{n_2\omega\sqrt{(n_1/n_2)^2\sin^2\theta - 1}}{c}z} \tag{124}$$

The transmitted light intensity decays as $e^{-\frac{2n_2\omega\sqrt{(n_1/n_2)^2\sin^2\theta-1}}{c}z}$. The decay length is the order of wavelength because $c/\omega = \lambda/2\pi$. The Poynting vector $\mathbf{S}$ in the z direction in the medium 2,

$$\begin{aligned}
\mathbf{z}\cdot\langle\mathbf{S}\rangle &= \frac{1}{2\mu_0\mu}\mathrm{Re}(\mathbf{E}\times\mathbf{B}''^{*})\cdot\mathbf{z} && (125)\\
&= \frac{1}{2\mu_0\mu\omega}\mathrm{Re}[\mathbf{E}\times(\mathbf{k}''\times\mathbf{E}'')^{*}]\cdot\mathbf{z} && (126)\\
&= \frac{1}{2\mu_0\mu\omega}\mathrm{Re}[\mathbf{k}''|\mathbf{E}''|^2 - \mathbf{E}''^{*}(\underbrace{\mathbf{k}''\cdot\mathbf{E}''}_{=0})\cdot\mathbf{z} && (127)\\
&= \frac{1}{2\mu_0\mu\omega}\mathrm{Re}(\underbrace{\mathbf{z}\cdot\mathbf{k}''}_{k''\cos\theta=\text{pure imaginary}}|\mathbf{E}''|^2) && (128)\\
&= 0 && (129)
\end{aligned}$$

Thereby the energy flux to $\hat{\mathbf{z}}$ direction in the medium 2 is zero. We call this exponential-decay wave as evanescent wave, and is used for some interface spectroscopies to detect species located at the evanescent field.

3.6.1 Phase Shift of the Total Internal Reflection Wave

For the total internal reflection the amplitudes of the incident wave and the reflected wave are the same but there is a phase shift between them.

$$\begin{aligned}
r_p &= \frac{n_2\cos\theta - n_1\cos\theta''}{n_2\cos\theta + n_1\cos\theta''} = \frac{a-ib}{a+ib} = \frac{a^2-b^2-2iab}{a^2+b^2} = e^{-i\delta_p} && (130)\\
a &= n_2\cos\theta, \quad b = n_1\sqrt{(n_1/n_2)^2\sin^2\theta - 1} && (131)\\
\tan(\delta_p) &= \frac{2ab}{a^2-b^2} && (132)\\
r_s &= \frac{n_1\cos\theta - n_2\cos\theta''}{n_1\cos\theta + n_2\cos\theta''} = \frac{c-id}{c+id} = \frac{c^2-d^2-2icd}{c^2+d^2} = e^{-i\delta_s} && (133)\\
c &= n_1\cos\theta, \quad d = n_2\sqrt{(n_1/n_2)^2\sin^2\theta - 1} && (134)\\
\tan(\delta_s) &= \frac{2cd}{c^2-d^2} && (135)
\end{aligned}$$

3.7 Metal Surface

For the metal surface the optical index becomes complex because some part of the light is absorbed by the electronic transition of metallic electrons at Fermi level.

$$\tilde{n}_2 = n_2 + i\kappa_2, \quad k'' = \tilde{n}_2\omega/c = (n_2 + i\kappa_2)\omega/c \qquad (136)$$

From the condition I,

$$n_1\sin\theta = \tilde{n}_2\sin\theta'' = (n_2 + i\kappa_2)\sin\theta'' \qquad (137)$$

Now θ'' is complex, and we define[13]

$$\begin{aligned}
\tilde{n}_2\cos\theta'' &\equiv u_2 + iv_2, \qquad \text{Here } u_2 \text{ and } v_2 \text{ are real.} && (138)\\
(u_2+iv_2)^2 &= \tilde{n}_2^2\cos^2\theta'' = \tilde{n}_2^2(1-\frac{n_1^2}{\tilde{n}_2^2}\sin^2\theta) = \tilde{n}_2^2 - n_1^2\sin^2\theta && (139)
\end{aligned}$$

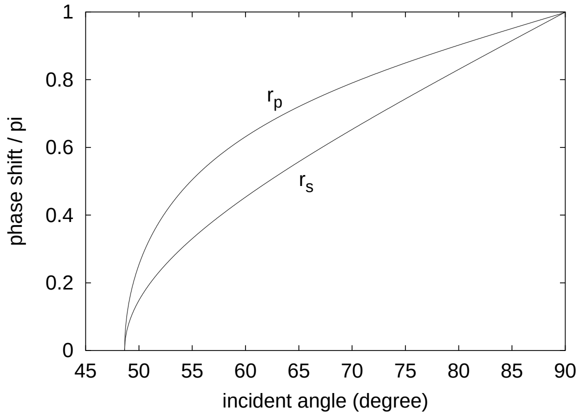

Figure 7: Phase shift of the TIR wave (He-Ne laser) from water|air interface.

For the real and imaginary parts of Eq.(139)

$$u_2^2 - v_2^2 = n_2^2 - \kappa_2^2 - n_1^2 \sin\theta^2 \tag{140}$$

$$2u_2 v_2 = 2n_2\kappa_2 \tag{141}$$

Then we can get

$$u_2^2 = \frac{n_2^2 - \kappa_2^2 - n_1^2\sin^2\theta + \sqrt{(n_2^2 - \kappa_2^2 - n_1^2\sin^2\theta)^2 + 4n_2^2k_2^2}}{2} \tag{142}$$

$$v_2^2 = \frac{-(n_2^2 - \kappa_2^2 - n_1^2\sin^2\theta) + \sqrt{(n_2^2 - \kappa_2^2 - n_1^2\sin^2\theta)^2 + 4n_2^2k_2^2}}{2} \tag{143}$$

For p wave,

$$r_p \equiv \rho_p e^{i\phi_p} = \frac{\tilde{n}_2\cos\theta - n_1\cos\theta''}{\tilde{n}_2\cos\theta + n_1\cos\theta''} = \frac{\tilde{n}_2^2\cos\theta - n_1\tilde{n}_2\cos\theta''}{\tilde{n}_2^2\cos\theta + n_1\tilde{n}_2\cos\theta''} \tag{144}$$

$$= \frac{(n_2^2 - \kappa_2^2 + 2in_2\kappa_2)\cos\theta - n_1(u_2 + iv_2)}{(n_2^2 - \kappa_2^2 + 2in_2\kappa_2)\cos\theta + n_1(u_2 + iv_2)} \tag{145}$$

$$\rho_p^2 = \left|\frac{(n_2^2 - \kappa_2^2)\cos\theta - n_1u_2 + i(2n_2\kappa_2\cos\theta - n_1v_2)}{(n_2^2 - \kappa_2^2)\cos\theta + n_1u_2 + i(2n_2\kappa_2\cos\theta + n_1v_2)}\right|^2 \tag{146}$$

$$= \frac{[(n_2^2 - \kappa_2^2)\cos\theta - n_1u_2]^2 + (2n_2\kappa_2\cos\theta - n_1v_2)^2}{[(n_2^2 - \kappa_2^2)\cos\theta + n_1u_2]^2 + (2n_2\kappa_2\cos\theta + n_1v_2)^2} \tag{147}$$

$$\tan\phi_p = \{[(n_2^2 - \kappa_2^2)\cos\theta + n_1u_2](2n_2\kappa_2\cos\theta - n_1v_2) - [(n_2^2 - \kappa_2^2)\cos\theta - n_1u_2] (2n_2\kappa_2\cos\theta + n_1v_2)\}/[(n_2^2 - \kappa_2^2)^2\cos^2\theta - n_1^2u_2^2 + 4n_2^2\kappa_2^2\cos\theta - n_1^2v_2^2]$$

$$= 2n_2\cos\theta\frac{2n_2u_2\kappa_2 - (n_2^2 - k_2^2)v_2}{(n_2^2 + \kappa_2^2)^2\cos^2\theta - n_1^2(u_2^2 + v_2^2)} \tag{148}$$

$$t_p = \tau_p e^{i\chi_p} = \frac{2n_1\cos\theta}{n_1\cos\theta'' + \tilde{n}_2\cos\theta} = \frac{2n_1\tilde{n}_2\cos\theta}{n_1\tilde{n}_2\cos\theta'' + \tilde{n}_2^2\cos\theta} \tag{149}$$

$$= \frac{2n_1n_2\cos\theta + i2n_1\kappa_2\cos\theta}{n_1u_2 + (n_2^2 - \kappa_2^2)\cos\theta + i(n_1v_2 + 2n_2\kappa_2\cos\theta)} \tag{150}$$

$$\tau_p^2 = 4n_1^2\cos^2\theta = \frac{n_2^2 + \kappa_2^2}{[n_1u_2 + (n_2^2 - \kappa_2^2)\cos\theta]^2 + (n_1v_2 + 2n_2\kappa_2\cos\theta)^2} \tag{151}$$

$$\tan\chi_p = 2n_1\cos\theta\frac{n_1\kappa_2u_2 + \kappa_2(n_2^2 - \kappa_2^2)\cos\theta - n_1n_2v_2 - 2n_2^2\kappa_2\cos\theta}{2n_2\cos\theta[n_1^2u_2 + n_1(n_2^2 - \kappa_2^2)\cos\theta + n_1\kappa_2v_2 + 2n_2\kappa_2^2\cos\theta]} \tag{152}$$

The t_p in the book "Born and Wolf, Principles of Optics (7th ed) p.575 Eqs.(14) and (15)"[13] may be wrong.

For s wave

$$r_s = \rho_s e^{i\phi_s} = \frac{n_1 \cos\theta - \tilde{n}_2 \cos\theta''}{n_1 \cos\theta + \tilde{n}_2 \cos\theta''} = \frac{n_1 \cos\theta - (u_2 + iv_2)}{n_1 \cos\theta + u_2 + iv_2} \quad (153)$$

$$\rho_s^2 = \left|\frac{n_1 \cos\theta - u_2 - iv_2}{n_1 \cos\theta + u_2 + iv_2}\right|^2 = \frac{(n_1 \cos\theta - u_2)^2 + v_2^2}{(n_1 \cos\theta + u_2)^2 + v_2^2} \quad (154)$$

$$\tan\phi_s = \frac{-2v_2 n_1 \cos\theta}{n_1^2 \cos^2\theta - u_2^2 - v_2^2} \quad (155)$$

$$t_s = \tau_s e^{i\chi_s} = \frac{2n_1 \cos\theta}{n_1 \cos\theta + \tilde{n}_2 \cos\theta''} = \frac{2n_1 \cos\theta}{n_1 \cos\theta + u_2 + iv_2} \quad (156)$$

$$\tau_s^2 = \left|\frac{2n_1 \cos\theta}{n_1 \cos\theta + u_2 + iv_2}\right|^2 = \frac{4n_1^2 \cos^2\theta}{(n_1 \cos\theta + u_2)^2 + v_2^2} \quad (157)$$

$$\tan\chi_s = -\frac{2v_2 n_1 \cos\theta}{2n_1^2 \cos^2\theta + 2u_2 n_1 \cos\theta} = -\frac{v_2}{n_1 \cos\theta + u_2} \quad (158)$$

For He-Ne laser (632.8 nm) the reflectance at the air|gold surface ($n = 0.181, \kappa = 2.99$) is shown in Fig.7. For IR light at 3100 nm the reflectance at the air|gold surface ($n = 1.728, \kappa = 19.2$) is shown in Fig. 8.

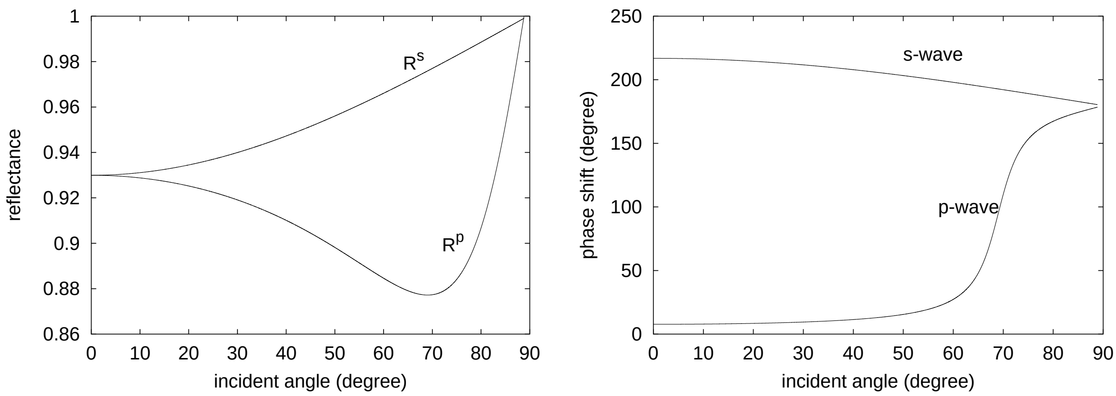

Figure 8: He-Ne laser (632.8 nm) reflection from air|Au surface

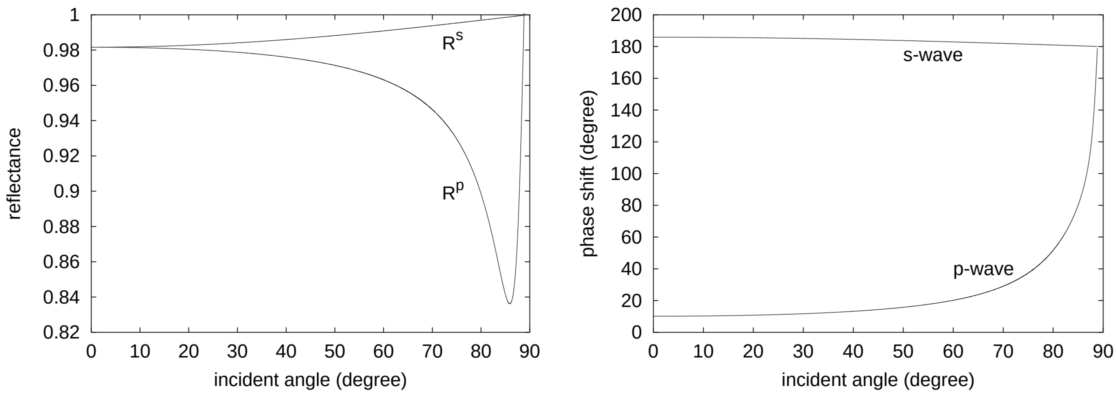

Figure 9: IR light (3100 nm) reflection from air|Au surface

The intensities of light in the z- and y-component per unit area on the Au surface becomes

$$
\begin{aligned}
(E_p^{\perp}/E_p)^2/\cos\theta &\equiv |\mathbf{E}_{0z}+\mathbf{R}_{0z}|^2/E_p^2/\cos\theta = |-E_p\sin\theta - R_p\sin\theta|^2/E_p^2/\cos\theta \\
&= |-E_p\sin\theta - r_pE_p\sin\theta|^2/E_p^2/\cos\theta \\
&= |-E_p\sin\theta - (\rho_p\cos\phi_p + i\rho_p\sin\phi_p)E_p\sin\theta_p|^2/E_p^2/\cos\theta \\
&= \sin\theta^2(1+2\rho_p\cos\phi_p+\rho_p^2)/\cos\theta \qquad (159) \\
(E_s^{\parallel}/E_s)^2/\cos\theta &\equiv |\mathbf{E}_{0y}+\mathbf{R}_{0y}|^2/E_s^2/\cos\theta \\
&= |E_s+R_s|^2/E_s^2/\cos\theta = |E_s+r_sE_s|^2/E_s^2\cos\theta \\
&= (1+2\rho_s\cos\phi_s+\rho_s^2)/\cos\theta \qquad (160)
\end{aligned}
$$

These equations give the basics of the surface sensitivity of the RAIRS(Reflection Absorption Infrared Spectroscopy) and Polarization-Modulation FTIR spectroscopy, and the angle dependence are shown in Fig.9. The 180 degree phase change of s-wave leads to destructive interference and no interaction with surface dynamic dipoles from molecular vibrations. [10] For the surface normal component of the p-wave the interference is constructive and it can excite the dynamic dipole perpendicular to the surface. The excitation is efficient for a higher angle of incidence.

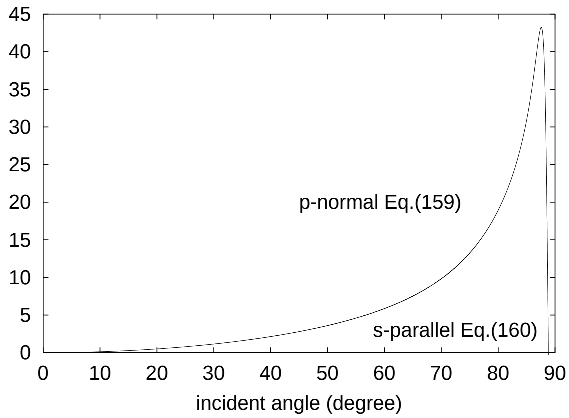

Figure 10: plots of $(E_p^{\perp}/E_p)^2/\cos\theta$ and $(E_s^{\parallel}/E_s)^2/\cos\theta$. The IR light is 3100 nm and the IR light is reflected from the air|Au surface. $(E_s^{\parallel}/E_s)^2/\cos\theta$ is negligible because the phase shift is almost 180 degree between the incident wave and the reflected wave.

4 Surface Plasmon

The electronic charges on metal boundary can perform coherent fluctuations which are called surface plasma oscillations. The fluctuations are confined at the boundary and vanishes both sides of the metal surface. This plasmon waves have p-character because the surface charge induce the discontinuity of the electric field in the surface normal z-direction, but s-waves has only E_y component (no E_z component).

Now we consider the air(medium 2)|metal(medium 1) surface where the electric fields are dumped both side of the interface.

Using a pure imaginary k_{z2} the electric and magnetic field in medium 2(air, $z > 0$)

[10] The surface parallel x-component (not shown here) of p-wave is also negligible.

can be given by

$$\mathbf{E}_2 = \begin{pmatrix} E_{x2} \\ 0 \\ E_{z2} \end{pmatrix} e^{i(k_{x2}x + k_{z2}z - \omega t)} \tag{161}$$

$$\mathbf{H}_2 = \begin{pmatrix} 0 \\ H_{y2} \\ 0 \end{pmatrix} e^{i(k_{x2}x + k_{z2}z - \omega t)} \tag{162}$$

Using a pure imaginary k_{z1} the electric and magnetic field in medium 1(metal, $z > 0$) can be given by

$$\mathbf{E}_1 = \begin{pmatrix} E_{x1} \\ 0 \\ E_{z1} \end{pmatrix} e^{i(k_{x1}x - k_{z1}z - \omega t)} \tag{163}$$

$$\mathbf{H}_1 = \begin{pmatrix} 0 \\ H_{y1} \\ 0 \end{pmatrix} e^{i(k_{x1}x - k_{z1}z - \omega t)} \tag{164}$$

From the Condition I, we can get

$$k_{x1} = k_{x2} = k_x \tag{165}$$

$$E_{x1} = E_{x2} \tag{166}$$

$$E_{z1} = E_{z2} \tag{167}$$

From condition IV,

$$H_{y1} = H_{y2} \tag{168}$$

$$\text{here we assume} \quad (J_s)_y \approx 0 \tag{169}$$

From condition III,

$$\tilde{\epsilon}_1 \epsilon_0 E_{z1} = \tilde{\epsilon}_2 \epsilon_0 E_{z2} \tag{170}$$

$$\text{here we assume} \quad \sigma_{12}(k_x, \omega) \ll D_{1z}, D_{2z} \tag{171}$$

From Eq.4 and $\mathbf{J} \approx 0$

$$\mathrm{rot}\mathbf{H} = \frac{\partial \mathbf{D}}{\partial t} \tag{172}$$

$$\mathrm{rot}\mathbf{H} = \begin{vmatrix} \mathbf{i} & \mathbf{j} & \mathbf{k} \\ \frac{\partial}{\partial x} & \frac{\partial}{\partial y} & \frac{\partial}{\partial z} \\ 0 & H_{yi} & 0 \end{vmatrix} = -\mathbf{i}\frac{\partial}{\partial z} H_{yi} + \mathbf{k}\frac{\partial}{\partial x} H_{yi} \tag{173}$$

From the $\mathbf{i}$ component of the above equation,

$$ik_{z1} H_{y1} = -i\omega \epsilon_0 \tilde{\epsilon}_1 E_{x1} \tag{174}$$

$$-ik_{z2} H_{y2} = -i\omega \epsilon_0 \tilde{\epsilon}_2 E_{x2} \tag{175}$$

$E_{x1} = E_{x2}$ then

$$\frac{k_{z1}}{\omega \epsilon_0 \tilde{\epsilon}_1} H_{y1} + \frac{k_{z2}}{\omega \epsilon_0 \tilde{\epsilon}_2} H_{y2} = 0 \tag{176}$$

$H_{y1} = H_{y2}$ then

$$\frac{k_{z1}}{\tilde{\epsilon}_1} + \frac{k_{z2}}{\tilde{\epsilon}_2} = 0 \tag{177}$$

From Eqs.(21) and (26)

$$\begin{aligned} k^2 &= k_x^2 + k_{zi}^2 = \tilde{\epsilon}_i \left(\frac{\omega}{c}\right)^2 && (178) \\ k_x^2 &= \tilde{\epsilon}_1 \left(\frac{\omega}{c}\right)^2 - k_{z1}^2 && (179) \\ k_x^2 &= \tilde{\epsilon}_2 \left(\frac{\omega}{c}\right)^2 - k_{z2}^2 \\ &= \tilde{\epsilon}_2 \left(\frac{\omega}{c}\right)^2 - \left(-\frac{\tilde{\epsilon}_2}{\tilde{\epsilon}_1} k_{z1}\right)^2 && (180) \end{aligned}$$

From the last two equations Eqs.(179) and (180).

$$k_x^2 = \left(\frac{\tilde{\epsilon}_1 \tilde{\epsilon}_2}{\tilde{\epsilon}_1 + \tilde{\epsilon}_2}\right) \left(\frac{\omega}{c}\right)^2 \tag{181}$$

$$\begin{aligned} k_{z1}^2 &= \left(\frac{\tilde{\epsilon}_1^2}{\tilde{\epsilon}_1 + \tilde{\epsilon}_2}\right) \left(\frac{\omega}{c}\right)^2 && (182) \\ k_{z2}^2 &= \left(\frac{\tilde{\epsilon}_2^2}{\tilde{\epsilon}_1 + \tilde{\epsilon}_2}\right) \left(\frac{\omega}{c}\right)^2 && (183) \end{aligned}$$

If we remind that $\tilde{\epsilon}_1 = \epsilon_1' + i\epsilon_1''$, $\tilde{\epsilon}_2 = \epsilon_2$

$$\begin{aligned} k_x^2 &= \left(\frac{\omega}{c}\right)^2 \frac{(\epsilon_1' + i\epsilon_1'')\epsilon_2}{(\epsilon_1' + i\epsilon_1'') + \epsilon_2} \\ &= \left(\frac{\omega}{c}\right)^2 \epsilon_2 \frac{\epsilon_1'(\epsilon_1' + \epsilon_2) + \epsilon_1''^2 + i[\epsilon_1''(\not\epsilon_1' + \epsilon_2) - \not\epsilon_1' \not\epsilon_1'']}{(\epsilon_1' + \epsilon_2)^2 + \epsilon_1''^2} && (184) \end{aligned}$$

If we assume $\epsilon_1'' < |\epsilon_1'|$

$$\begin{aligned} \mathrm{Re}(k_x) &= \frac{\omega}{c} \left(\frac{\epsilon_1' \epsilon_2}{\epsilon_1' + \epsilon_2}\right)^{1/2} && (185) \\ \mathrm{Im}(k_x) &= \frac{\omega}{c} \left(\frac{\epsilon_1' \epsilon_2}{\epsilon_1' + \epsilon_2}\right)^{3/2} \frac{\epsilon_1''}{2\epsilon_1'^2} && (186) \end{aligned}$$

The surface plasmon decay in x-direction can be evaluated from $\mathrm{Im}(k_x)$ because the intensity decreased as $\exp[-2\mathrm{Im}(k_x)x]$. The decay length L_{12} may be obtained as

$$L_{12} = [2\mathrm{Im}(k_x)]^{-1} = \frac{c}{\omega} \left(\frac{\epsilon_1' \epsilon_2}{\epsilon_1' + \epsilon_2}\right)^{-3/2} \frac{\epsilon_1'^2}{\epsilon_1''} \tag{187}$$

For the water|metal interface the decay lengths L_{12} are 6.4 μm for gold (16.6 μm for air|gold surface), 12.3 μm for silver, and 5.5 μm for aluminum. The decay length L_{12} is the key parameter to carry out a SPR imaging measurements [11]. In addition there is a temporal decay in ω, please refer the Raether's book for details[1].

[11] この議論から SPR において横方向のイメージングの分解能はマイクロメータサイズ以上であることがわかる。L_{12} の小さいアルミニウムを使って、生きた細胞を SPR イメージングで観測した例も報告されている。[15]

The dispersion relation k_x vs ω become close to the light line $\sqrt{\epsilon_2}\omega/c$ at small k_x, because in the limit that $\omega \to 0, \epsilon_1' >> \epsilon_2$. At large k_x the denominator of Eq.(185) becomes zero

$$\epsilon_1' + \epsilon_2 = 0 \tag{188}$$

For simple metals the dielectric constant is given by the plasma frequency ω_p[16] [12]

$$\epsilon_1' = 1 - \frac{\omega_p^2}{\omega^2} \tag{189}$$

From Eqs.(188) and (189) the surface plasma frequency ω_{sp} may be obtained as

$$\omega_{\rm sp} = \omega_p \frac{1}{\sqrt{1+\epsilon_2}} \tag{190}$$

In Fig.10 we plot the dispersion relation Eq.(185).

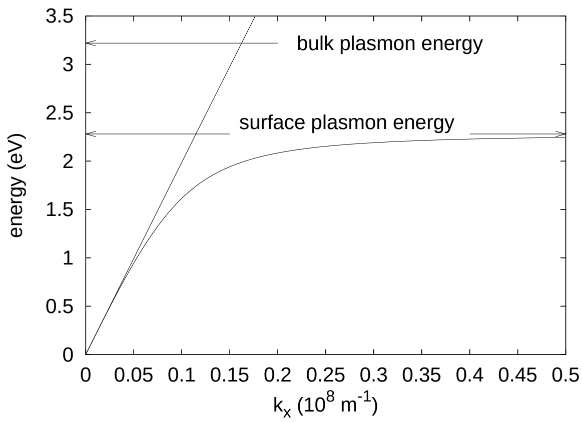

Figure 11: Surface plasmon dispersion $\omega(k_x)$ on gold surface. The vertical axis is scaled as $\hbar\omega$ (eV). The straight solid line in the figure shows the light line $k_x = \sqrt{\epsilon_2}\omega/c$. The energy of bulk plasmon is 3.22 eV, and that of surface plasmon is 2.28 eV and shown as the arrows in the figure.

In the z-direction the electric field of the surface plasmon decays as $E_z \propto e^{-|k_{zi}||z|}$. If we assume $\epsilon_1'' < |\epsilon_1'|$ again,

$$k_{z1}^2 \approx \left(\frac{\epsilon_1'^2}{\epsilon_1' + \epsilon_2}\right)\left(\frac{\omega}{c}\right)^2 \tag{191}$$

$$k_{z2}^2 \approx \left(\frac{\epsilon_2^2}{\epsilon_1' + \epsilon_2}\right)\left(\frac{\omega}{c}\right)^2 \tag{192}$$

$\epsilon_1' + \epsilon_2 < 0$ then k_{zi} is purely imaginary. For He-Ne laser light (632.8 nm) on the gold surface

$$1/{\rm Re}(k_{z1})({\rm metal}) = 32 \text{ nm}, \quad 1/{\rm Re}(k_{z2})({\rm air}) = 285 \text{ nm} \tag{193}$$

From the $\mathbf{k}$ component of rot$\mathbf{H} = \partial\mathbf{D}/\partial t$ [cf. Eq.(173)]

$$\frac{\partial H_{y1}}{\partial x} = ik_{x1}H_{y1} = -i\omega\epsilon_0\tilde{\epsilon_1}E_{z1} \tag{194}$$

$$\frac{\partial H_{y2}}{\partial x} = ik_{x2}H_{y2} = -i\omega\epsilon_0\tilde{\epsilon_2}E_{z2} \tag{195}$$

[12]電子線を金属に照射して電子線のエネルギー損失を測定するとその金属のプラズマ振動数が測定される。表面・界面にのみ存在する表面プラズモンも反射電子線のエネルギー損失から測定される。

From the **i** component of Eqs.(172-173) and Eq.(194)

$$H_{y1} = -\frac{\omega\epsilon_0\tilde{\epsilon_1}E_{x1}}{k_{z1}} = -\frac{\omega\epsilon_0\tilde{\epsilon_1}E_{z1}}{k_{x1}} \tag{196}$$

$$\frac{E_{z1}}{E_{x1}} = \frac{k_{x1}}{k_{z1}} \tag{197}$$

$$H_{y2} = \frac{\omega\epsilon_0\tilde{\epsilon_2}E_{x2}}{k_{z2}} = -\frac{\omega\epsilon_0\tilde{\epsilon_2}E_{z2}}{k_{x2}} \tag{198}$$

$$\frac{E_{z2}}{E_{x2}} = -\frac{k_{x2}}{k_{z2}} \tag{199}$$

(200)

5 Excitation of Surface Plasmon by Light

5.1 ATR (Attenuated Total Reflection) Coupler Method

We will consider the situation that the light is reflected from a metal surface covered with a dielectric medium ($\epsilon_{pr} > 1$) , e.g. with a BK7 half cylinder glass prism (n=1.515 at 633 nm) or SF10 glass prism (n=1.723 at 643.8 nm). The x and z components of the wavevector in the prism are given by

$$k_x^{pr} = \sqrt{\epsilon_{pr}}\frac{\omega}{c}\sin\theta_{pr} = n_{pr}\frac{\omega}{c}\sin\theta_{pr} \tag{201}$$

$$k_z^{pr} = \sqrt{\epsilon_{pr}}\frac{\omega}{c}\cos\theta_{pr} = n_{pr}\frac{\omega}{c}\cos\theta_{pr} \tag{202}$$

Here pr means the prism.

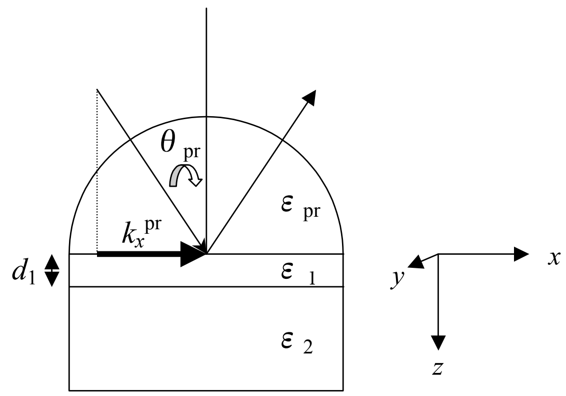

Figure 12: Schematic diagram of ATR coupler: Kretschmann-Raether type

The resonance condition of the light in the prism with the surface plasmon at metal(1)|air(2) interface (Kretschmann-Raether configuration) is [13]

$$k_x^{pr} = k_x^{sp} \tag{203}$$

[13]ATR カプラーには、プリズム | 金属薄膜 | 試料系の Kretschmann-Raether 型とプリズム | 薄層（波長程度の厚み）試料 | 金属の Otto 型がある。Otto 型は薄層の gap 調整が必要であり、Kretschmann-Raether 型が主に使用されている。ただし、Kretschmann-Raether 型では膜厚（50nm 程度）を慎重に制御して金属をガラスに真空蒸着しなくてはならない。また、ガラスに金を蒸着したサンプルを電気化学的な環境下で電位をかけると、金が剥がれるため (3-mercaptopropyl)trimethoxysilane(MPS) をガラス | 金のバインダーにした基板を用いている。(cf. Appendix) ATR カプラーで表面プラズモンを光により励起できることを最初に示したのは Otto であるが [4]、Otto は Kretschmann-Raether 型のカプラーでは SPR は起きないと主張して、それが間違いであることが明らかになったためか (?!)、その後 SPR の表舞台に出てくることはなかった。

$$\sqrt{\epsilon_{pr}}\frac{\omega}{c}\sin\theta_{pr} \quad = \quad \sqrt{\frac{\tilde{\epsilon}_1\tilde{\epsilon}_2}{\tilde{\epsilon}_1+\tilde{\epsilon}_2}}\left(\frac{\omega}{c}\right) \tag{204}$$

Here we use Eq.(181) for k_x^{sp}.

5.1.1 Prisim|Metal|Medium Three-Layer Model

The reflectivity $R_{pr|1|2}$ may be given by Frensel's equations of the prism|metal|air three-layer system.

$$r_{ik}^p = \frac{\tilde{n}_k\cos\theta_i - \tilde{n}_i\cos\theta_k}{\tilde{n}_k\cos\theta_i + \tilde{n}_i\cos\theta_k} = \frac{\tilde{n}_k\frac{k_{zi}}{k_i} - \tilde{n}_i\frac{k_{zk}}{k_k}}{\tilde{n}_k\frac{k_{zi}}{k_i} + \tilde{n}_i\frac{k_{zk}}{k_k}} = \frac{\frac{\tilde{n}_k k_{zi}c}{\tilde{n}_i\omega} - \frac{\tilde{n}_i k_{zk}c}{\tilde{n}_k\omega}}{\frac{\tilde{n}_k k_{zi}c}{\tilde{n}_i\omega} + \frac{\tilde{n}_i k_{zk}c}{\tilde{n}_k\omega}} \tag{205}$$

$$= \frac{\frac{k_{zi}}{\tilde{n}_i^2} - \frac{k_{zk}}{\tilde{n}_k^2}}{\frac{k_{zi}}{\tilde{n}_i^2} + \frac{k_{zk}}{\tilde{n}_k^2}} = \frac{k_{zi}/\tilde{\epsilon}_i - k_{zk}/\tilde{\epsilon}_k}{k_{zi}/\tilde{\epsilon}_i + k_{zk}/\tilde{\epsilon}_k} \tag{206}$$

$$r_{ki}^p = -r_{ik}^p \tag{207}$$

For transmission

$$t_{ik}^p = \frac{\tilde{n}_i}{\tilde{n}_k}(1+r_{ik}^p) \tag{208}$$

$$t_{ki}^p = \frac{\tilde{n}_k}{\tilde{n}_i}(1+r_{ki}^p) = \frac{\tilde{n}_k}{\tilde{n}_i}(1-r_{ik}^p) \tag{209}$$

$$t_{ik}^p t_{ki}^p = (1+r_{ik}^p)(1-r_{ik}^p) \tag{210}$$

The total reflection of the three-layer model becomes

$$R = |r_{\mathrm{pr}12}^p|^2 = \left|\frac{r_{\mathrm{pr}1}^p + r_{12}^p e^{2ik_{z1}d_1}}{1 + r_{\mathrm{pr}1}^p r_{12}^p e^{2ik_{z1}d_1}}\right|^2 \tag{211}$$

$$r_{ik}^p = \frac{\tilde{n}_k\cos\theta_i - \tilde{n}_i\cos\theta_k}{\tilde{n}_k\cos\theta_i + \tilde{n}_i\cos\theta_k} = \frac{\cos\theta_i/\tilde{n}_i - \cos\theta_k/\tilde{n}_k}{\cos\theta_i/\tilde{n}_i + \cos\theta_k/\tilde{n}_k} \tag{212}$$

$$n_{pr}\sin\theta_{pr} = \tilde{n}_1\sin\theta_1 = \tilde{n}_2\sin\theta_2$$

$$\tilde{n}_k\cos\theta_k = \tilde{n}_k(1-\sin^2\theta_k)^{1/2} = \tilde{n}_k(1-n_{pr}^2\sin^2\theta_{pr}/\tilde{n}_k^2)^{1/2} = (\tilde{n}_k^2 - n_{pr}^2\sin^2\theta_{pr})^{1/2}$$

$$r_{ik}^p = \frac{(\tilde{\epsilon}_i - n_{pr}^2\sin^2\theta_{pr})^{1/2}/\tilde{\epsilon}_i - (\tilde{\epsilon}_k - n_{pr}^2\sin^2\theta_{pr})^{1/2}/\tilde{\epsilon}_k}{(\tilde{\epsilon}_i - n_{pr}^2\sin^2\theta_{pr})^{1/2}/\tilde{\epsilon}_i + (\tilde{\epsilon}_k - n_{pr}^2\sin^2\theta_{pr})^{1/2}/\tilde{\epsilon}_k} \tag{213}$$

$$r_{\mathrm{pr}1}^p = \frac{\cos\theta_{pr}/n_{pr} - (\tilde{\epsilon}_1 - n_{pr}^2\sin^2\theta_{pr})^{1/2}/\tilde{\epsilon}_1}{\cos\theta_{pr}/n_{pr} + (\tilde{\epsilon}_1 - n_{pr}^2\sin^2\theta_{pr})^{1/2}/\tilde{\epsilon}_1} \tag{214}$$

The above equation for R can be understood by considering

$$\begin{aligned}
r_{\mathrm{pr}12}^p &= \frac{r_{\mathrm{pr}1}^p + r_{12}^p e^{2ik_{z1}d_1}}{1 + r_{\mathrm{pr}1}^p r_{12}^p e^{2ik_{z1}d_1}} \qquad (215)\\
&\approx (r_{\mathrm{pr}1}^p + r_{12}^p e^{2ik_{z1}d_1})(1 - r_{\mathrm{pr}1}^p r_{12}^p e^{2ik_{z1}d_1} + (r_{\mathrm{pr}1}^p)^2(r_{12}^p)^2 e^{4ik_{z1}d_1} - ....)\\
&= r_{\mathrm{pr}1}^p + r_{12}^p e^{2ik_{z1}d_1} - (r_{\mathrm{pr}1}^p)^2 r_{12}^p e^{2ik_{z1}d_1}\\
&\quad - r_{\mathrm{pr}1}^p (r_{12}^p)^2 e^{4ik_{z1}d_1} + (r_{\mathrm{pr}1}^p)^3 (r_{12}^p)^2 e^{4ik_{z1}d_1} + ...\\
&= r_{\mathrm{pr}1}^p + (1 - r_{\mathrm{pr}1}^p)^2 r_{12}^p e^{2ik_{z1}d_1} + r_{\mathrm{pr}1}^p[(r_{\mathrm{pr}1}^p)^2 - 1](r_{12}^p)^2 e^{4ik_{z1}d_1} + ...
\end{aligned}$$

$$
\begin{aligned}
&= r^p_{\rm pr1} + \underbrace{(1+r^p_{\rm pr1})r^p_{12}(1-r^p_{\rm pr1})}_{t^p_{\rm pr1}r^p_{12}t^p_{\rm 1pr}} e^{2ik_{z1}d_1} \\
&\quad + \underbrace{(1+r^p_{\rm pr1})r^p_{12}(-r^p_{\rm pr1})r^p_{12}(1-r^p_{\rm pr1})}_{t^p_{\rm pr1}r^p_{12}r^p_{\rm 1pr}r^p_{12}t^p_{\rm 1pr}} e^{4ik_{z1}d_1} \\
&= r^p_{\rm pr1} + t^p_{\rm pr1}r^p_{12}t^p_{\rm 1pr}e^{2ik_{z1}d_1} + t^p_{\rm pr1}r^p_{12}r^p_{\rm 1pr}r^p_{12}t^p_{\rm 1pr}e^{4ik_{z1}d_1} \qquad (216)
\end{aligned}
$$

phase factor $\quad k_{z1}d_1 = k_1(d_1\cos\theta_1)$ is optical path length. (217)

$$
\begin{aligned}
k_{z1}d_1 &= k_1 d_1 \cos\theta_1 = \tilde{n}_1 \frac{\omega}{c} d_1 \left(1 - \frac{n^2_{pr}}{\tilde{n}^2_1}\sin^2\theta_{pr}\right)^{1/2} \\
&= \frac{\omega}{c} d_1 (\tilde{\epsilon}_1 - n^2_{pr}\sin^2\theta_{pr})^{1/2} \qquad (218)
\end{aligned}
$$

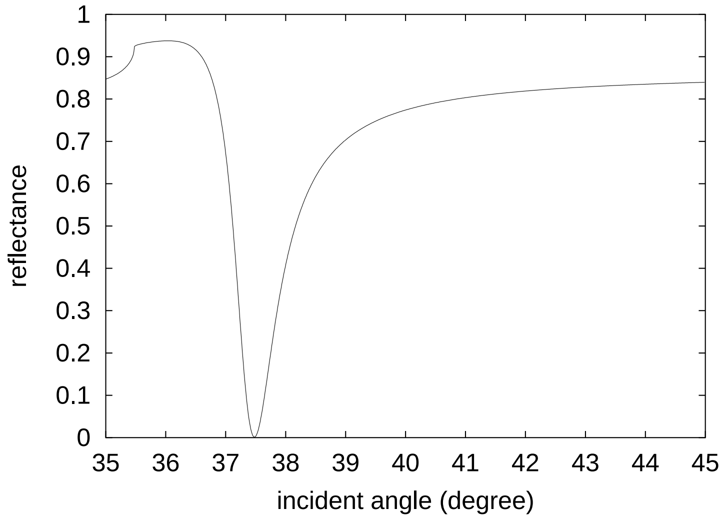

Figure 13: SPR curve for SF10(n = 1.723)|gold(50nm, $\tilde{n}_1$ = 0.1726+i3.4218) |air(n = 1.0) for He-Ne laser light (633 nm).

The FORTRAN program to get the SPR curve by Eq.(211) is

```
c234567-- spr_angle_3layer.f ---
c     complex calculation
      implicit real*8 (a-h,o-z)

      complex*16 e1,rpr1,r12,rpr12,rpr12c,alpha,ref
      complex*16 aaa,fukso,e2

      c=2.99792458d8
      hbar=6.5822d-16
      pi=acos(-1.0d0)
c     ------ air ----
      e2=dcmplx(1.0d0,0.0d0)
c     ----- SF10 633 nm
      enpr=1.723d0
c     ----- gold 633 nm
      e1n=0.1726d0
```

```
      e1k=3.4218d0
      e1r=e1n**2-e1k**2
      e1i=2.0d0*e1n*e1k
      e1=dcmplx(e1r,e1i)
c     ---- gold thickness (m)
      d1=50.0d-9
c
      ramd=633.0d-9
      omega=2.0d0*pi/ramd*c
      fukso=dcmplx(0.0d0,1.0d0)
      write (6,*) ramd,omega,hbar*omega
c     --------- angle scan ----------
      ang0=35.0d0
      ang1=45.0d0
      do i=1, 1001
       theta=(ang0+dble(i-1)/1000.0d0*(ang1-ang0))/180.0d0*pi
       rpr1=(cos(theta)/enpr -
     &       sqrt(e1-enpr**2*sin(theta)**2)/e1)
     &      / (cos(theta)/enpr +
     &      sqrt(e1-enpr**2*sin(theta)**2)/e1)

       r12=( sqrt(e1-enpr**2*sin(theta)**2)/e1 -
     &       sqrt(e2-enpr**2*sin(theta)**2)/e2 )
     &     / ( sqrt(e1-enpr**2*sin(theta)**2)/e1 +
     &         sqrt(e2-enpr**2*sin(theta)**2)/e2 )
       aaa=2.0d0*omega/c*d1*sqrt(e1-enpr**2*sin(theta)**2)
       alpha=aaa*fukso
       rpr12=(rpr1+ r12*exp(alpha))/(1.0d0+rpr1*r12*exp(alpha))
       rpr12c=conjg(rpr12)
       ref=rpr12*rpr12c
       write (6,*) theta/pi*180.0d0,dble(ref)
      enddo
      end
```

The calculated results are shown in Fig. 12. At resonance or $R = 0$ the power of the SPs is lost by internal absorption in the metal. This loss is compensated by the power of the incoming light. Both have to be equal in the steady state.

If the reflectivity R has lowest value, the intensity of the electromagnetic field reaches its maximum at the metal surface. For 600 nm light **the maximum enhancement of the electric field intensity** is ca. 200 for silver film (60 nm thickness), 30 for gold film, 40 for aluminum film, and 7 for copper film, respectively[1].

5.2 General solution of N-layer model. [F. Abelès, Ann. Phys. (Paris) 5, (1950) 596. W. N. Hansen, J. Opt. Soc. Amer. 58 (1968) 380.]

The tangential fields at the first boundary $z = z_1 = 0$ are related to those at the final boundary $z = z_{N-1}$ by

$$\begin{bmatrix} U_1 \\ V_1 \end{bmatrix} = M_2 M_3 ... M_{N-1} \begin{bmatrix} U_{N-1} \\ V_{N-1} \end{bmatrix} = M \begin{bmatrix} U_{N-1} \\ V_{N-1} \end{bmatrix} \tag{219}$$

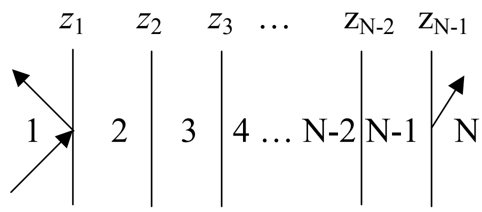

Figure 14: N-layer model for SPR measurement.

For p-wave at boundary k,

$$U_k = H_y^T + H_y^R \tag{220}$$

$$V_k = E_x^T + E_x^R \tag{221}$$

and

$$M_k = \begin{bmatrix} \cos\beta_k & -i\sin\beta_k/q_k \\ -iq_k\sin\beta_k & \cos\beta_k \end{bmatrix} \tag{222}$$

$$\text{Here } q_k = (\mu_k/\tilde{\epsilon_k})^{1/2}\cos\theta_k \tag{223}$$

$$\mu_k \cong 1$$

$$q_k \cong (1/\tilde{\epsilon_k})^{1/2}\cos\theta_k = \frac{(\tilde{\epsilon_k} - n_1^2\sin^2\theta_1)^{1/2}}{\tilde{\epsilon_k}} \tag{224}$$

$$\beta_k = \frac{2\pi}{\lambda_0}\tilde{n}_k\cos\theta_k(z_k - z_{k-1}) = (z_k - z_{k-1})\frac{2\pi}{\lambda_0}(\tilde{\epsilon}_k - n_1^2\sin^2\theta_1)^{1/2} \tag{225}$$

The reflection and transmission coefficient for p-wave (TM) is

$$r^p = \frac{(M_{11} + M_{12}q_N)q_1 - (M_{21} + M_{22}q_N)}{(M_{11} + M_{12}q_N)q_1 + (M_{21} + M_{22}q_N)} \tag{226}$$

$$M_{ij} = \left(\prod_{k=2}^{N-1} M_k\right)_{ij}, \quad i, j = 1, 2 \tag{227}$$

$$R_p = |r_p|^2 \tag{228}$$

$$r_p = R_p^{1/2}e^{i\phi_p^r} \tag{229}$$

$$\phi_p^r = \arg(r^p) \tag{230}$$

$$t_H^p = \frac{2q_1}{(M_{11} + M_{12}q_N)q_1 + (M_{21} + M_{22}q_N)} \tag{231}$$

$$t_E^p = \frac{\mu_N n_1}{\mu_1\tilde{n}_N}t_H^p \tag{232}$$

$$T_p = \frac{\mu_N \mathrm{Re}(\tilde{n}_N\cos\theta_N/\tilde{n}_N^2)}{\mu_1 n_1\cos\theta_1/n_1^2}|t_H^p|^2 \tag{233}$$

$$\phi_p^t = \arg(t_E^p) \tag{234}$$

For s-wave (TE) the above equations hold except

$$q_k = \sqrt{\frac{\tilde{\epsilon_k}}{\mu_k}}\cos\theta_k \tag{235}$$

In this sense these equations are easy to calculate the multilayer optical problem.

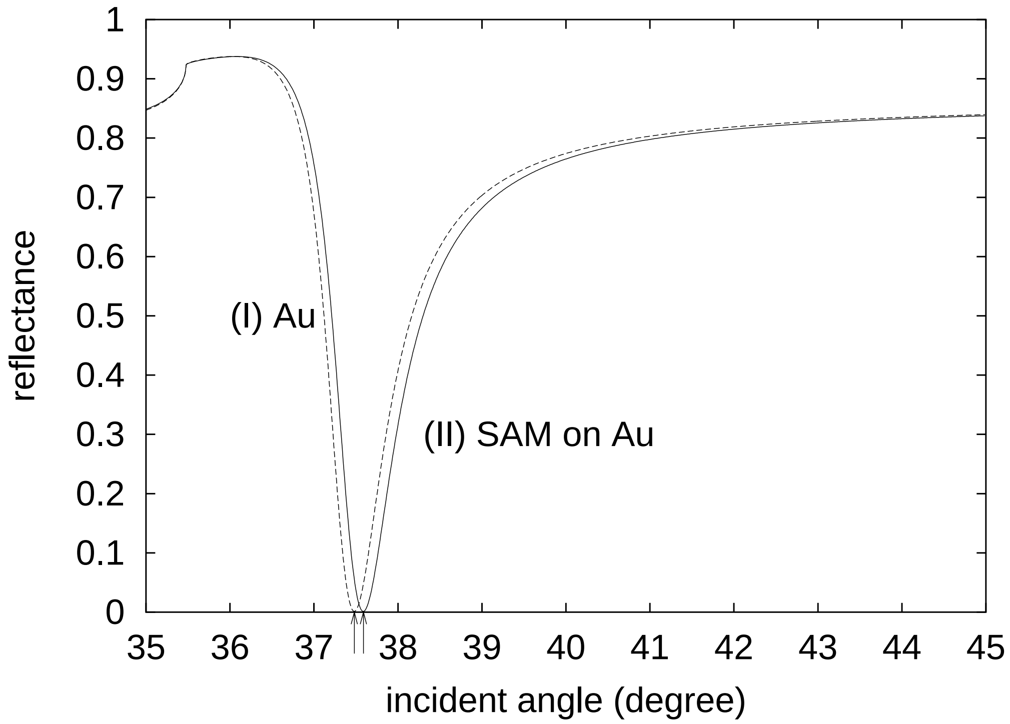

Figure 15: SPR curves for (I) the SF10 glass prism(n=1.723)|Au($n+ik = 0.1726+i3.4218$, 50nm)|Air(n=1.0) and (II) the SF10 prism|Au(50nm)|SAM(n=1.61245, 1nm)|Air systems.

The SPR resonance calculation FORTRAN program for N-layer system is given in the following, and the results for the 4-layer system [prism|gold|Self-Assmbled-Monolayer(SAM, 1 nm thickness)|Air] is shown in Fig. 14. **The SAM film thickness of 1 nm is clearly seen as the shift of the SPR angle.**

```
c234567-- spr_angle_Nlayer.f ---
c     1 | 2 | 3 ...  N-2|N-1|N :N layer system
c     complex calculation
      implicit real*8 (a-h,o-z)

      parameter (nlay=10)
      complex*16 e(nlay) , em(nlay,2,2) ,emtot(2,2)
      complex*16 emtot1(2,2)
      dimension en(nlay), ek(nlay), d(nlay)
      complex*16 beta,q,rp,q1,qn,ref,tp,tra
      complex*16 fukso

      c=2.99792458d8
      hbar=6.5822d-16
      pi=acos(-1.0d0)
c     ------- N layer ----
      nlayer=4
c     ------ air ----
      en(4)=1.d0
      ek(4)=0.0d0
```

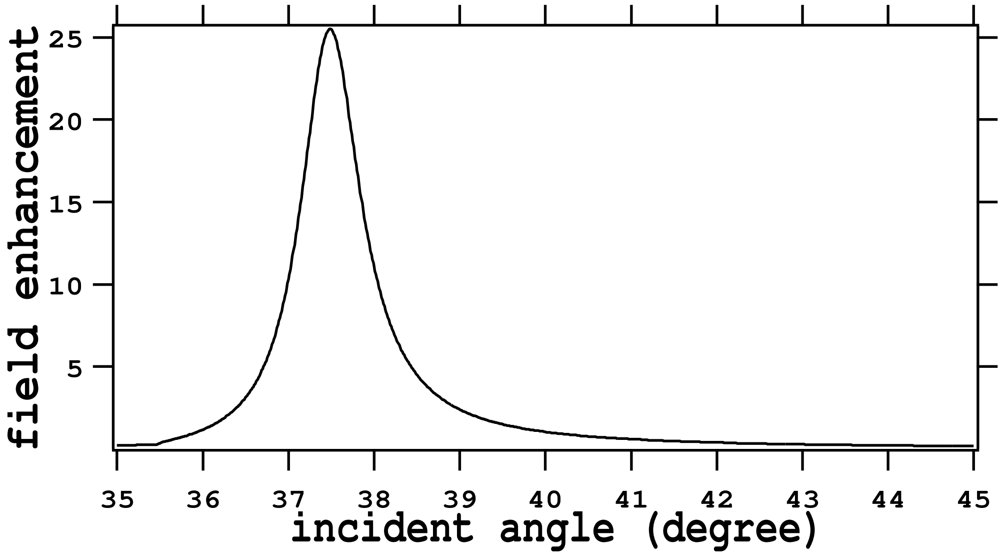

Figure 16: Field enhancement factor $|t_{\mathrm{h}}^{p}|^2$ for the the SF10 prism|Au(50nm)|SAM(n=1.61245, 1nm)|Air system.

```
      er=en(4)**2-ek(4)**2
      ei=2.0d0*en(4)*ek(4)
      e(4)=dcmplx(er,ei)
c     ----- SF10 633 nm
      en(1)=1.723d0
      ek(1)=0.0d0
      er=en(1)**2-ek(1)**2
      ei=2.0d0*en(1)*ek(1)
      e(1)=dcmplx(er,ei)
c     ----- gold 633 nm
      en(2)=0.1726d0
      ek(2)=3.4218d0
      er=en(2)**2-ek(2)**2
      ei=2.0d0*en(2)*ek(2)
      e(2)=dcmplx(er,ei)
c     ---- gold thickness (m)
      d(2)=50.0d-9
c     ------ SAM -----------
      en(3)=1.61245
      ek(3)=0.0d0
      er=en(3)**2-ek(3)**2
      ei=2.0d0*en(3)*ek(3)
      e(3)=dcmplx(er,ei)
c     ----- SAM thickness ---
      d(3)=1.0d-9
c
      ramd=633.0d-9
      omega=2.0d0*pi/ramd*c
      fukso=dcmplx(0.0d0,1.0d0)
      write (6,*) ramd,omega,hbar*omega
```

```
c     --------- angle scan ----------
      ang0=35.0d0
      ang1=45.0d0
      do i=1, 1001
       theta=(ang0+dble(i-1)/1000.0d0*(ang1-ang0))/180.0d0*pi
       q1=sqrt(e(1)-en(1)**2*sin(theta)**2)/e(1)
       qn=sqrt(e(nlayer)-en(1)**2*sin(theta)**2)/e(nlayer)
       do j=2, nlayer-1
        beta=d(j)*2.0d0*pi/ramd*sqrt(e(j)-en(1)**2*sin(theta)**2)
        q=sqrt(e(j)-en(1)**2*sin(theta)**2)/e(j)
        em(j,1,1)=cos(beta)
        em(j,1,2)=-fukso*sin(beta)/q
        em(j,2,1)=-fukso*sin(beta)*q
        em(j,2,2)=cos(beta)
       enddo
        emtot(1,1)=dcmplx(1.0d0,0.0d0)
        emtot(2,2)=dcmplx(1.0d0,0.0d0)
        emtot(1,2)=dcmplx(0.0d0,0.0d0)
        emtot(2,1)=dcmplx(0.0d0,0.0d0)
       do j=2, nlayer-1
        emtot1(1,1)=em(j,1,1)
        emtot1(1,2)=em(j,1,2)
        emtot1(2,1)=em(j,2,1)
        emtot1(2,2)=em(j,2,2)
        emtot=matmul(emtot,emtot1)
       enddo

       rp=( (emtot(1,1)+emtot(1,2)*qn)*q1 -
     &      (emtot(2,1)+emtot(2,2)*qn) )
     &    / ( (emtot(1,1)+emtot(1,2)*qn)*q1 +
     &      (emtot(2,1)+emtot(2,2)*qn) )
       tp=2.0d0*q1/( (emtot(1,1)+emtot(1,2)*qn)*q1 +
     &      (emtot(2,1)+emtot(2,2)*qn) )

       rp=( (emtot(1,1)+emtot(1,2)*qn)*q1 -
     &      (emtot(2,1)+emtot(2,2)*qn) )
     &    / ( (emtot(1,1)+emtot(1,2)*qn)*q1 +
     &      (emtot(2,1)+emtot(2,2)*qn) )
       tp=2.0d0*q1/( (emtot(1,1)+emtot(1,2)*qn)*q1 +
     &      (emtot(2,1)+emtot(2,2)*qn) )

       ref=rp*conjg(rp)
       enh=tp*conjg(tp)
       tra=tp*conjg(tp)/cos(theta)*en(1)*dble(qn)
       write (6,*) theta/pi*180.0d0,dble(ref),enh
c     write (6,*) theta/pi*180.0d0,dble(ref),dble(tra)
      enddo
      end
```

6 Acknowledgement

The author would like to thank for Mr. A. Shirakami for his great contribution to the startup of the SPR study in our laboratory. The author also thank Prof. R. Corn, Prof. T. Kakiuchi and Dr. D. Hobora for helpful discussions on this subject.

7 Appendix

In Fig.16 the phase shifts of the reflected wave(He-Ne laser light) are shown in the case of Air($n = 1$) →Water($n = 1.332$)(top figure) and Water→Air(bottom figure). For the case of Water→Air the critical angle for total reflection is 48.66 degree and the phase shift is shown in Fig.6.

References

[1] H. Raether. *Surface Plasmons on Smooth and Rough Surface and on Gratings.* Springer-Verlag, Berlin, 1988.

[2] R. H. Ritchie. Plasma losses by fast electrons in thin films. *Phys. Rev.*, 106:874–881, 1957.

[3] R. W. Wood. On a remarkable case of uneven distribution of light in a diffraction grating spectrum. *Phil. Mag. Ser. 6*, 4:396–402, 1902.

[4] A. Otto. Excitation of surface plasma waves in silver by the method of frustrated total reflection. *Z. Physik*, 216:398–410, 1968.

[5] H. Raether E. Kretschmann. Radaitive decay of non-radiative surface plasmons excited by light. *Z. Naturforsch.*, 23A:2135–2136, 1968.

[6] J. G. Gordon II and J. D. Swalen. The effect of thin organic films on the surface plasma resonace on gold. *Opt. Commun.*, 22:374–376, 1977.

[7] C. Nylander B. Liedberg and I. Lundstrom. Surface plasmon resonance for gas and biosensing. *Sensers and Acutuators*, 4:299–304, 1983.

[8] B. L. Frey R. Corn D. G. Hanken, C. E. Jordan. Surface plasmon reasonance measurements of ultrathin organic films at electrode surfaces. *Electroanal. Chem.*, 20:141–225, 1998.

[9] W. Knoll. Interfaces and thin films as seen by bound electromagnetic waves. *Annu. Rev. Phys. Chem.*, 49:569–638, 2000.

[10] R. Corn J. M. Brockman, B. P. Nelson. Surface plasmon reasonance imaging measurements of ultrathin organic films. *Annu. Rev. Phys. Chem.*, 51:41–63, 2000.

[11] D. M. Kolb. The study of solid-liquid interfaces by surface plasmon polariton excitation. In V. M. Agranvich and D. L. Mills, editors, *Surface Polaritons*, chapter 8, pages 299–329. North-Holland, Amsterdam, 1982.

[12] V. Scheumann Z. Zizlsperger J. Mack G. Jung A. Badia, S. Arnold and W. Knoll. Probing the elecrochemical deposition and/or desorption of self-assembled and electropolymerizable organic thin film by surface plasmon spectroscopy and atomic force microscopy. *Sensors and Actuators B*, 54:145–165, 1999.

[13] M. Born and E. Wolf. *Principles of Optics (7th expanded edition).* Cambridge University Press, Cambridge, 1999.

[14] E. Hecht. *Optics.* Addison-Wesley, San Francisco, 2002.

[15] S. Herminghaus M. Riedel P. Leiderer U. Weiland K.-F. Giebel, C. Bechinger and M. Bastmeyer. Imaging of cell/substrate contacs of living cells with surface plasmon resonance microscopy. *BioPhys. J.*, 76:509–516, 1999.

[16] C. Kittel. *Introduction to Solid State Physics (7th edition).* Wiley, New York, 1996.

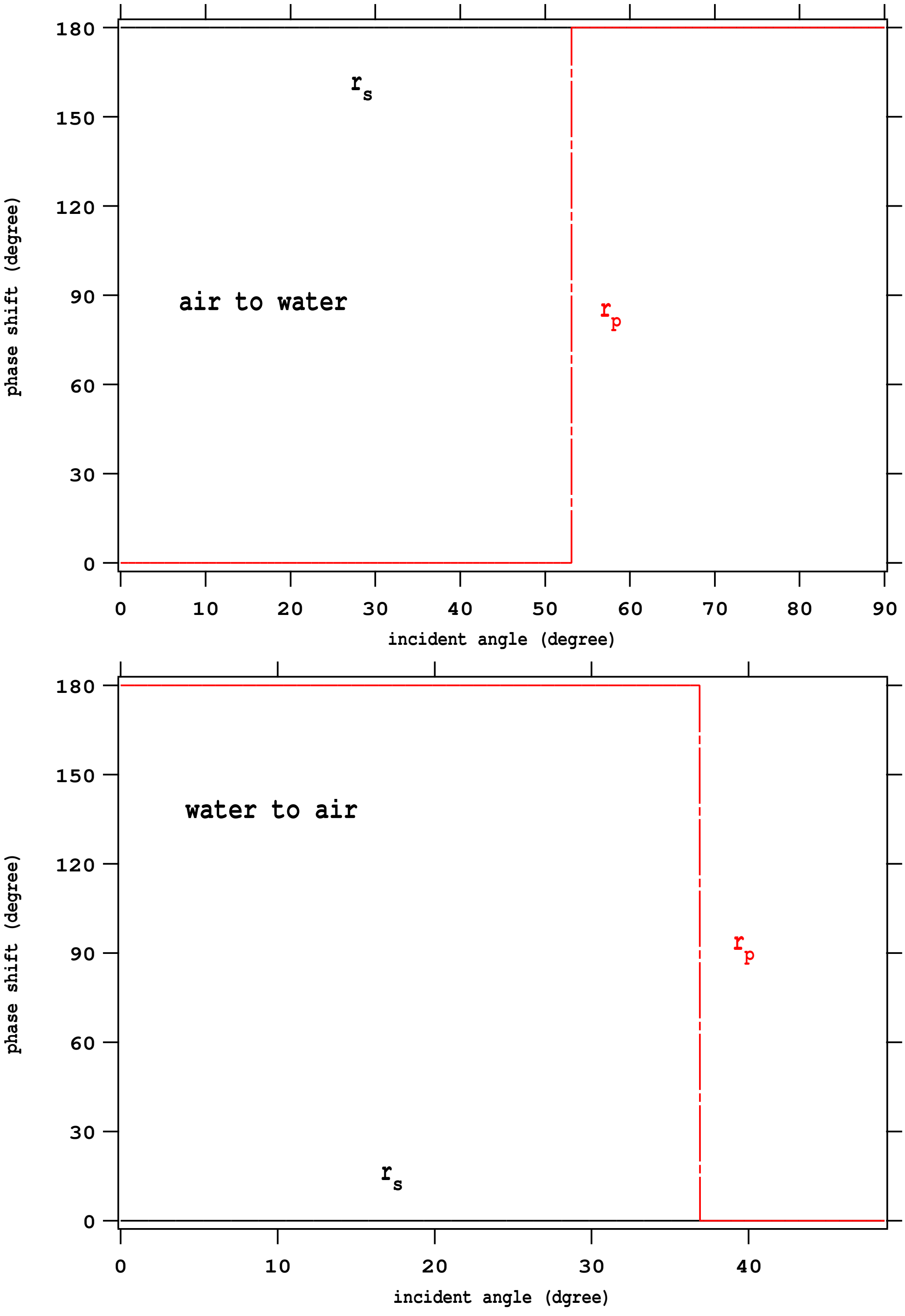

Figure 17: Phase shifts of the reflected wave(He-Ne laser light) are shown in the case of Air($n = 1$) →Water($n = 1.332$)(top figure) and Water→Air(bottom figure). For the case of Water→Air the critical angle for total reflection is 48.66 degree and the phase shift is shown in Fig.6.

In Fig.17 schematic diagram of light reflection from black film is shown. When the incident angle is small, the phase shift of s wave is π for OC and zero for OAB and the phase shift of p wave is zero for OC and π for OAB.(Please see Fig.16) If the film thickness d is much smaller than the wavelength/4, the interference between OC and wave from B become destructive.(Please note that the formulation is shown in the inset of Fig.17). Then we can see no light from thin film like lipid bilayer or soap bubble.

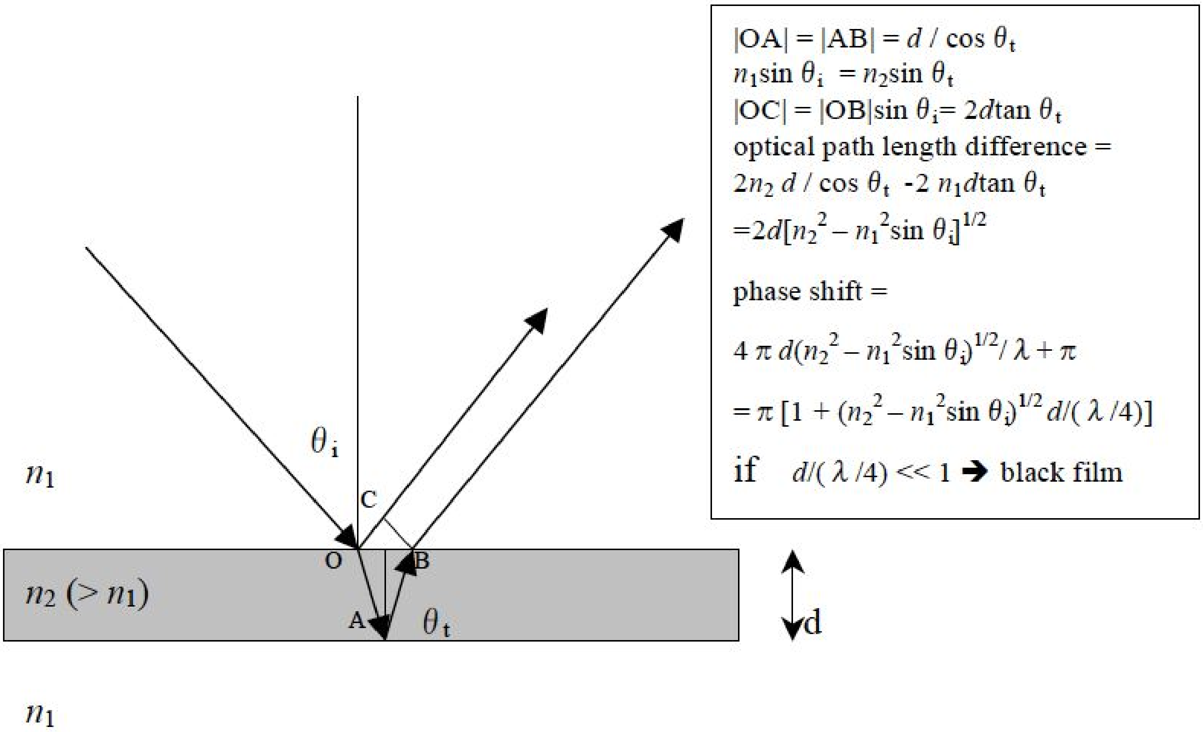

Figure 18: Schematic diagram of light reflection for black film. When the incident angle is small, the phase shift of s wave is π for OC and zero for OAB and the phase shift of p wave is zero for OC and π for OAB.(Please see Fig.16) If the film thickness d is much smaller than the wavelength/4, the interference between OC and wave from B become destructive. Please note that the formulation is shown in the inset. Then we can see no light from thin film like lipid bilayer or soap bubble.

Appendix

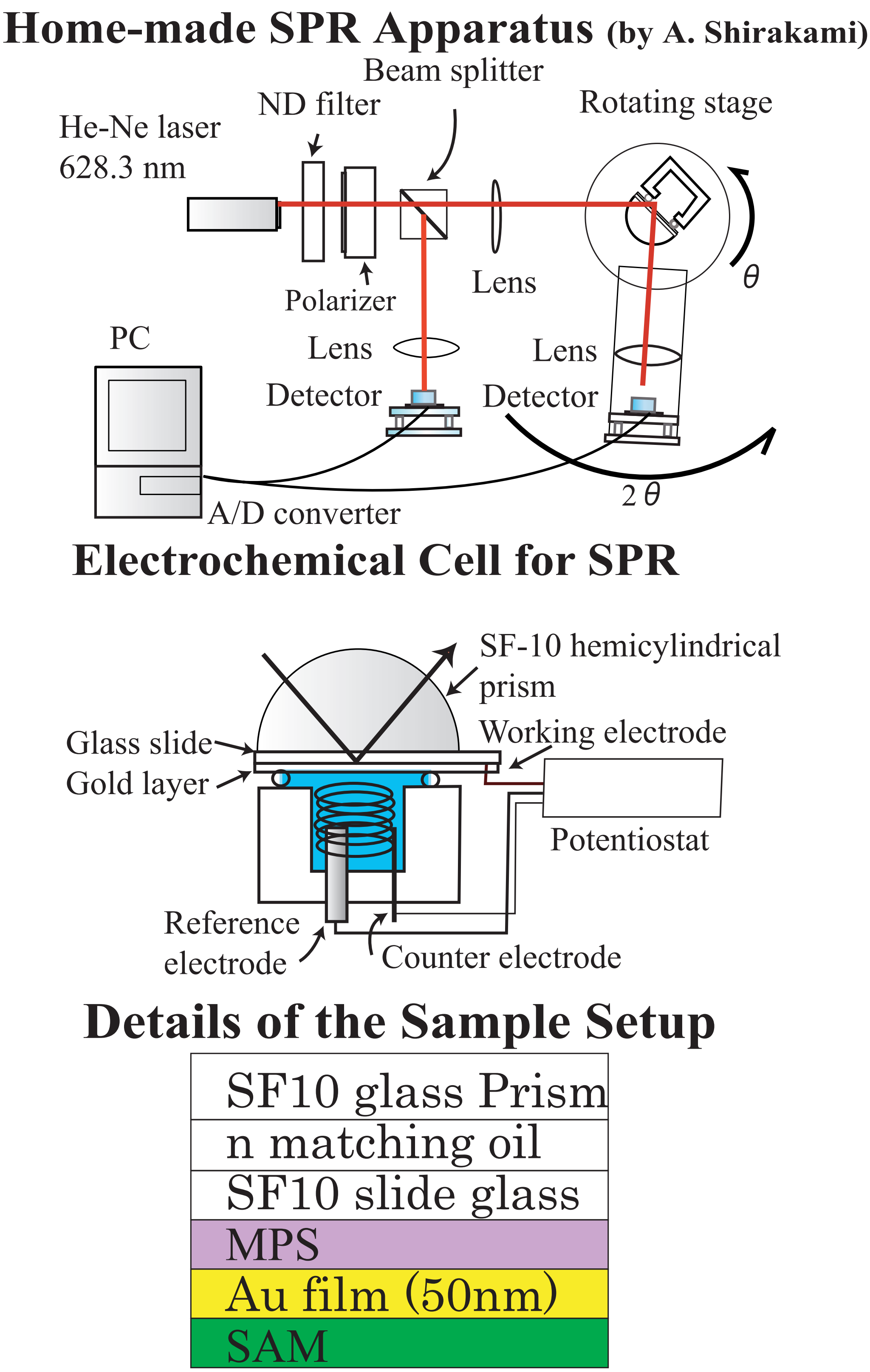

Figure 19: